Journal of Nonlinear Modeling and Analysis
Volume 4, Number 2, June 2022, 245–276
http://jnma.ca; http://jnma.ijournal.cn
DOI:10.12150/jnma.2022.245

A Family of Variable Step-size Meshes Fourth-order Compact Numerical Scheme for (2+1)-dimensions Burger's-Huxley, Burger's-Fisher and Convection-diffusion Equations

Navnit Jha[1,†] and Madhav Wagley[2]

Abstract Existing numerical schemes, maybe high-order accurate, are obtained on uniformly spaced meshes and challenges to achieve high accuracy in the presence of singular perturbation parameter, and nonlinearity remains left on nonuniformly spaced meshes. A new scheme is proposed for nonlinear 2D parabolic partial differential equations (PDEs) that attain fourth-order accuracy in xy-space and second-order exact in the temporal direction for uniform and nonuniform mesh step-size. The method proclaims a compact character using nine-point single-cell finite-difference discretization on a nonuniformly spaced spatial mesh point. A description of splitting compact operator form to the convection-dominated equation is obtained for implementing alternating direction implicit scheme. The procedure is examined for consistency and stability. The scheme is applied to linear and nonlinear 2D parabolic equations: convection-diffusion equations, Burger's-Huxley, Burger's-Fisher and coupled Burger's equation. The technique yields the tridiagonal matrix and computed by the Thomas algorithm. Numerical simulations with linear and nonlinear problems corroborate the theoretical outcome.

Keywords Nonlinear parabolic partial differential equations (PDEs), Two-dimensions Burger's-Huxley equation, Boussinesq equation, Convection-diffusion equation, Compact-scheme, Stability, Errors and numerical order.

MSC(2010) 65M12, 65M06.

1. Introduction

The parabolic partial differential equations (PDEs) appear to model ample physical phenomena in fluid flow, acoustic waves, mass transfer, groundwater, air pollution, chemical separation, shock wave, logistic population growth and nuclear reactor theory [4, 27, 28, 41]. In the past, Cole [7] described the analytic solution method for one-dimension Burger's equation, appearing in a turbulence model and weak

[†]the corresponding author.
Email address: navnitjha@sau.ac.in (N. Jha), madhav.wagley@famu.edu (M. Wagley)
[1]Department of Mathematics, South Asian University, Akbar Bhawan, 110021 New-Delhi, India
[2]Department of Mathematics, Florida A&M University, Tallahassee, Florida, USA

nonstationary shock wave. Subsequently, a two-dimensional form of Burger's equation was reported by Fletcher [14] and Bhatt [2]. There are two essential variants to Burger's equation, namely Burger's Fisher and Burger's Huxley model, that occupy a prominent place in mathematical physics and many application areas. The 2D Burger's Fisher equation occurs in turbulence gas dynamics and plasma physics. It has diffusion transport and reaction behavior from the Fisher equation and convective phenomenon from the Burgers equation. The two-dimensional Burger's Fisher equation takes the form

$$\epsilon\left(\frac{\partial^2 W}{\partial x^2}+\frac{\partial^2 W}{\partial y^2}\right)=\frac{\partial W}{\partial t}+aW^n\left(\frac{\partial W}{\partial x}+\frac{\partial W}{\partial y}\right)+bW\left(W^n-1\right), \tag{1.1}$$

and Burger's Huxley equation appearing in nerve propagation, population genetics is represented by

$$\epsilon\left(\frac{\partial^2 W}{\partial x^2}+\frac{\partial^2 W}{\partial y^2}\right)=\frac{\partial W}{\partial t}+aW^n\left(\frac{\partial W}{\partial x}+\frac{\partial W}{\partial y}\right)+W\left(W^n-1\right)\left(W^n-\sigma\right). \tag{1.2}$$

The 2D Burger's Fisher equation (1.1) and Burger's Huxley equations (1.2) can be represented in the following mildly nonlinear equation

$$\epsilon\left(\frac{\partial^2 W}{\partial x^2}+\frac{\partial^2 W}{\partial y^2}\right)=\psi\left(x,y,t,W,\frac{\partial W}{\partial x},\frac{\partial W}{\partial y},\frac{\partial W}{\partial t}\right),(x,y,t)\in\Omega\times(0,T),\Omega\in\mathbf{R^2} \tag{1.3}$$

along with initial and boundary data

$$W(x,y,0)=\phi(x,y), \tag{1.4}$$
$$W(0,y,t)=G_1(y,t),W(1,y,t)=G_2(y,t), \tag{1.5}$$
$$W(0,x,t)=F_1(x,t),W(x,1,t)=F_2(y,t). \tag{1.6}$$

The nonlinearity of first-order partial derivatives appearing in the parabolic PDEs (1.3) makes it difficult to determine the analytic solution. Various computational techniques, namely finite-difference, homotopy perturbation, finite-element, adomain decomposition, finite-volume and spectral methods, were presented to analyze mildly nonlinear convection dominated diffusion models approximately. The solution schemes using compact discretizations in the finite-difference have been described in the past [17, 18, 33]. Noye and Tan [37] presented a stable third-order accurate in space and second-order accurate in time, implicit weighted compact discretization to the 2D constant-coefficient linear advection-diffusion. A high-order uniform meshes compact formulation for solving time-dependent linear convection dominated diffusion using the boundary value method was presented by Dehghan and Mohebbi [8]. A monotone finite difference discretization to singularly perturbed parabolic PDEs and analysis of their uniform convergence was described by Clavero and Jorge [6]. A lattice Boltzmann model to compute 2D Burger's equation and its stability was discussed by Duan and Liu [9]. The analysis of a high-order difference scheme for convection dominated diffusion problems has been recently obtained in [1, 36, 38]. Recently, the one-dimensional Burgers equation has been described by Jiwari [23]. It is long-familiar that the analytic solution of singularly perturbed nonlinear parabolic PDEs for an arbitrary selection of the function ψ is not possible, and numerical solution by classical finite-difference or finite-element method may portray multiple characters or rapid change of solution in a specific

region [32]. The computational method consists of replacing the partial derivatives by equivalent finite differences at the appropriate mesh-point. The popularity of the compact finite-difference discretization is attributed to its generality and simplicity of applications, and it has been used for mathematical modeling of a different process [40]. The quasi-variable mesh discretizes the domain of a model into the finite number of mesh locations. The approximate solution to the recursive equations is computed at the limited mesh locations defined by the mesh line intersection. The procedure provides a point-wise approximation of parabolic PDEs by repetitive application of truncated series expansion. However, it remains a challenge to develop simple, stable and computationally efficient discretization schemes for solving such two-dimensions PDEs in the presence of small parameter (singular perturbation) and nonlinearity. Many high accuracy schemes are developed using a uniform mesh network, and it lacks in determining precise solution values, when the model possesses boundary layer character or singularity. The approximate solution values may be inaccurate, if standard upwind and second central-difference operators on uniformly spaced meshes are considered unless the mesh step-length is sufficiently small. The choice of many mesh points results in a large sparse matrix, and computing large size matrix consumes immense CPU time. Due to the rapid change of solution values in a small zone, the difference scheme defined on non-uniformly spaced meshes found more suitable for analyzing solution behavior everywhere in the integration domain. It can be achieved by putting more mesh points in the small zone having the frequent changing solution, and fewer mesh points in the subdomain with smooth solution values. Along these lines, it was conceivable to achieve a uniform circulation of local truncation errors and discretization errors [12]. In addition to non-uniformly distributed mesh points, the high-order discretization of PDEs also plays an important role that yields optimal solution values in short computing time. We are making use of the minimum number of mesh stencils essential in the discrete replacement to the highest order derivatives and also yield a block-tridiagonal matrix system. The solution to such a matrix system is numerically stable and memory-efficient, requiring short computing time. Moreover, the Jacobian matrix occurs with a low condition number. As a result, among several possible high-order mechanisms, minimum meshes involvement in the discretization process is preferred, and such a scheme is classified as compact and listed among the stable ones. Therefore, we aim to develop an implicit nine-point compact scheme for the numerical treatment of nonlinear 2D parabolic PDEs (1.3) on a non-uniformly spaced mesh network. The general scheme can be considered for solving Burger's Fisher, Burger's Huxley or convection dominated diffusion equation with appropriate boundary and initial values.

The paper has been prepared in the following structure: In Section 2, we introduce a new mesh topology that results in the equal magnitude of truncation error of high-order discretization in a uniform and variable mesh spacing. In Section 3, we construct compact operators that estimate the first- and second-order partial derivatives corresponding to convection and diffusion terms. We discretize the simplest form of time-dependent PDEs that are fourth-order exact in xy-space, and offer second-order accuracy with t-axis on a variable mesh spacing and on uniformly distributed meshes. An algorithmic presentation of the two-level high-order implicit compact scheme is presented in Section 4, and detailed derivations are obtained in Section 5. In Section 6, the description of an alternating direction implicit scheme for the 2D linear time-dependent convection dominated diffusion equation is pre-

sented. The new compact scheme is extended to 2D coupled Burger's equation, and detailed stability theory is elaborated in Section 7. In Section 8, numerical simulations in terms of solution accuracies and computational convergence order are shown, illustrating the robustness and efficiency of the new scheme that falls in the range of optimal accuracy. In the end, we have added new findings, difficulties, and possible extensions.

2. Mesh topology and compact operators

Variable spacing in the sequence of spatial mesh points is commonly employed to enhance accuracies of approximate solution values for the discretized parabolic PDEs whose exact solutions are not smooth. Since variable mesh spacing affects the order of truncation errors, the arbitrary choice of mesh points may not result in the compact scheme of optimal accuracy. One such consideration is to choose the next mesh step-size as a nonlinear combination of the previous mesh step-size. The implementation of such a variable mesh network offers an identical order of truncation error as derived from a uniformly spaced mesh point. In the present mathematical model, the spatial domain $\Omega = \{(x, y) : 0 \leq x, y \leq 1\}$ is partitioned into the finite mesh points $\{(x_l, y_m), 0 \leq l \leq L+1, 0 \leq m \leq M+1\}$. The temporal mesh points $t_j = j\delta t, 0 \leq j \leq J$, to the time-domain $0 \leq t \leq T$, are considered with the fixed time-step $\delta t = T/J$. Let $\delta x_l = x_l - x_{l-1}, l = 1(1)L+1$, and $\delta y_m = y_m - y_{m-1}, m = 1(1)M+1$ be the step-sizes along x- and y-coordinate directions. The next mesh-step sizes are defined by $\delta x_{l+1} = \delta x_l(1+\alpha\delta x_l), l = 1(1)L$, and $\delta y_{m+1} = \delta y_m(1+\beta\delta y_m), m = 1(1)M$. Here, α and β are mesh-expansion ratios to quasi-variable meshes along x-, and y-directions respectively, and $0 \leq \alpha, \beta \leq 1$. If we choose $\alpha = 0$, and $\beta = 0$, the meshing scheme generates uniformly distributed meshes along x- and y-directions respectively. The numerical mesh generation can be realized by making use of appropriate normalization parameters δx_1 and δy_1. To the subsequent mesh-step sizes, that is, $\delta x_{l+1} = \delta x_l(1 + \alpha\delta x_l/\delta x_1), l = 1(1)L$, and $\delta y_{m+1} = \delta y_m(1+\beta\delta y_m/\delta y_1), m = 1(1)M$. Given the length of diffusion domain in x- and y-directions, we know that $\sum_{l=1}^{L+1} \delta x_l = x_{L+1} - x_0$ and $\sum_{m=1}^{M+1} \delta y_m = y_{M+1} - y_0$. As a result, for the known value of mesh-expansion parameters α, β and corner mesh points $\{x_0, x_{L+1}\} \times \{y_0, y_{M+1}\}$, we can generate the quasi-variable mesh step-size and the corresponding internal mesh points according to the following formula

$$
\begin{aligned}
&a_1 = 1, a_2 = 1+\alpha, a_l = a_{l-1}(1+\alpha a_{l-1}), l = 3(1)L+1,\\
&a_1 = 1, a_2 = 1+\alpha, a_l = a_{l-1}(1+\alpha a_{l-1}), l = 3(1)L+1,\\
&\delta x_1 = (x_{L+1} - x_0)/\sum_{l=1}^{L+1} a_l, \quad \delta y_1 = (x_{M+1} - y_0)/\sum_{m=1}^{M+1} b_m,\\
&\delta x_2 = \delta x_1 a_2, \quad \delta x_l = \delta x_1 a_l, \quad l = 3(1)L+1, \quad x_l = x_{l-1} + \delta x_l, l = 1(1)L,\\
&\delta y_2 = \delta y_1 b_2, \delta y_m = \delta y_1 b_m, m = 3(1)M+1, y_m = y_{m-1} + \delta y_m, m = 1(1)M.
\end{aligned}
$$

For $\alpha \geq 0$, we find that $\delta x_{l+1} \geq \delta x_l$ for all l, thus, the mesh-step sequence $\{\delta x_l\}_{l=1}^{L+1}$ is monotonic increasing and therefore, there exists a Lagrange interpolating polynomial $\mathcal{H}$ of degree $L+1$ such that $\mathcal{H}(x_l^*) = x_l, \ l = 0(1)L+1$, where $\{x_l^* = l\delta x, l = 0, \ldots, L+1, \ \delta x = (x_{L+1} - x_0)/(L+1)\}$ is the uniformly spaced mesh points in the interval $[x_0, x_{L+1}]$ along x-direction. By using Mean value theorem,

one obtains

$$\delta x_{l+1} = x_{l+1} - x_l = \mathcal{H}(x^*_{l+1}) - \mathcal{H}(x^*_l) = \delta x \mathcal{H}'(x^{**}), x^{**} \in (x^*_l, x^*_{l+1}). \tag{2.1}$$

The maximal length of the non-uniform mesh steps is bounded by the maximal value of $\mathcal{H}'(x)$, and it exists since $\mathcal{H}(x)$ is continuously differentiable. As a result, $\delta x_{l+1} \leq w\delta x$, $w = \max_{x\in[x_0,x_{L+1}]}|\mathcal{H}'(x)|$. This implies that $\max_{l=0(1)L}|\delta x_{l+1}| \leq w\delta x$, and if we denote $\delta\mathbf{x} = [\delta x_1, \delta x_2, \ldots, \delta x_{L+1}]$, then, we find $\|\delta\mathbf{x}\|$. Then, we find $\|\delta\mathbf{x}\|_\infty \leq w\delta x = w(x_{L+1} - x_0)/(L+1) < w/L$. Thus, one obtains that

$$\|\delta\mathbf{x}\|_\infty = O(\delta x) = O(1/L) \text{ and } \|\delta\mathbf{x}\|_\infty \to 0 \text{ as } L \to \infty. \tag{2.2}$$

Similarly, we can prove that the mesh points sequence $\{y_m\}_{m=1}^{M+1}$ in the y-space is well defined, and the limiting value of mesh-steps diminishes for a sufficiently large value of M. In the past, such type of quasi-variable mesh network for solving mathematical models appearing in digital electrochemistry and wind-driven ocean circulation has been discussed in [5,43,44,47]. Bieniasz [3] and Jha et al., [19–21] has described a quasi-variable mesh network combined with compact finite-difference discretization to one- and two-dimensions boundary value problems.

3. Compact operators and basic scheme

At the mesh-point (x_l, y_m, t_j), we refer to $W^j_{l,m}$ as the exact values. Whereas, $w^j_{l,m}$ refers to the approximate values to the solution $W(x, y, t)$. In the underlying analysis, we shall denote the evaluation of $\partial W/\partial x, \partial W/\partial y, \partial^2 W/\partial x^2, \partial^2 W/\partial y^2$ at the mesh-point (x_l, y_m, t_j) by the symbols $W^{x^j}_{l,m}$, $W^{y^j}_{l,m}$, $W^{xx^j}_{l,m}$, and $W^{yy^j}_{l,m}$ respectively. We need to construct the compact operators that approximate the first- and second-order spatial derivatives and first-order temporal derivative. The construction will be based on a minimal stencil, which is required to discretize the maximum order partial derivatives present inside the parabolic PDEs. That is, one central mesh-point (x_l, y_m, t_j) and four neighboring mesh points $(x_{l\pm1}, y_m, t_j)$, $(x_l, y_{m\pm1}, t_j)$. With the help of three-point linear combination in each coordinate direction, we can estimate

$$\begin{bmatrix}\mathcal{A}_x\\ \mathcal{B}_x\end{bmatrix} W^j_{l,m} = \begin{bmatrix} -\dfrac{1+\alpha\delta x_l}{2+\alpha\delta x_l} & \dfrac{\alpha\delta x_l}{1+\alpha\delta x_l} & \dfrac{1}{(1+\alpha\delta x_l)(2+\alpha\delta x_l)} \\ \dfrac{2}{2+\alpha\delta x_l} & \dfrac{-2}{1+\alpha\delta x_l} & \dfrac{2}{(1+\alpha\delta x_l)(2+\alpha\delta x_l)} \end{bmatrix} \begin{bmatrix} W^j_{l-1,m}\\ W^j_{l,m}\\ W^j_{l+1,m}\end{bmatrix} \tag{3.1}$$

and

$$\begin{bmatrix}\mathcal{A}_y\\ \mathcal{B}_y\end{bmatrix} W^j_{l,m} = \begin{bmatrix} -\dfrac{1+\beta\delta y_m}{2+\beta\delta y_m} & \dfrac{\beta\delta y_m}{1+\beta\delta y_m} & \dfrac{1}{(1+\beta\delta y_m)(2+\beta\delta y_m)} \\ \dfrac{2}{2+\beta\delta y_m} & \dfrac{-2}{1+\beta\delta y_m} & \dfrac{2}{(1+\beta\delta y_m)(2+\beta\delta y_m)} \end{bmatrix} \begin{bmatrix} W^j_{l,m-1}\\ W^j_{l,m}\\ W^j_{l,m+1}\end{bmatrix}. \tag{3.2}$$

The finite Taylor's series expansions to (3.1) and (3.2) yields

$$\begin{bmatrix}\mathcal{A}_x\\ \mathcal{B}_x\end{bmatrix} W^j_{l,m} = \begin{bmatrix}\delta x_l W^{x^j}_{l,m}\\ \delta x_l^2 W^{xx^j}_{l,m}\end{bmatrix} + \begin{bmatrix}O(\delta x_l^3)\\ O(\delta x_l^4)\end{bmatrix} \tag{3.3}$$

and

$$\begin{bmatrix}\mathcal{A}_y\\ \mathcal{B}_y\end{bmatrix} W^j_{l,m} = \begin{bmatrix}\delta y_m W^{y^j}_{l,m}\\ \delta y^2_m W^{yy^j}_{l,m}\end{bmatrix} + \begin{bmatrix}O(\delta y^3_m)\\ O(\delta y^4_m)\end{bmatrix}. \tag{3.4}$$

Therefore, at the j^{th} time level, the new difference operators provide second-order accuracy to the first- and second-order spatial partial derivatives on a quasi-variable mesh network, since

$$W^{x^j}_{l,m} = \delta x_l^{-1}\mathcal{A}_x W^j_{l,m} + O(\delta x_l^2), \quad W^{y^j}_{l,m} = \delta y_m^{-1}\mathcal{A}_y W^j_{l,m} + O(\delta y_m^2) \tag{3.5}$$

and

$$W^{xx^j}_{l,m} = \delta x_l^{-2}\mathcal{B}_x W^j_{l,m} + O(\delta x_l^2), \quad W^{yy^j}_{l,m} = \delta y_m^{-2}\mathcal{B}_y W^j_{l,m} + O(\delta y_m^2). \tag{3.6}$$

Note that these three-point operators are commutative, and if $\alpha = 0$, we have $\mathcal{A}_x = 2\mu_x\delta_x$, $\mathcal{B}_x = \delta_x^2$, where $\mu_x W_{l,m} = (W^j_{l+1/2,m} + W^j_{l-1/2,m})/2$ is the averaging operator and $\delta_x W^j_{l,m} = W^j_{l+1/2,m} + W^j_{l-1/2,m}$ is the first central-difference operator in x-direction. Similarly, for $\beta = 0$, we have $\mathcal{A}_y = 2\mu_y\delta_y$ and $\mathcal{B}_y = \delta_y^2$, where μ_y and δ_y are the averaging and the first central-difference operators, which are respectively in y-direction. Likewise, we can derive compact operators at $(j+1)^{th}$-time level. The straight implementation of the operators (3.1) and (3.2) to the nonlinear parabolic PDEs (1.3) yields the difference equations

$$\begin{aligned}\epsilon(\delta x_l^{-2}\mathcal{B}_x + \delta y_m^{-2}\mathcal{B}_y)W^j_{l,m} = \psi(x_l, y_m, t_j, W^j_{l,m}, \delta x_l^{-1}\mathcal{A}_x W^j_{l,m},\\ \delta y_m^{-1}\mathcal{A}_y W^j_{l,m}, \delta t\overline{W}^{t^j}_{l,m}) + O(\delta x_l^2 + \delta y_m^2 + \delta t),\end{aligned} \tag{3.7}$$

where $\overline{W}^{t^j}_{l,m}$ is the approximated first-order partial derivative using forward difference along time direction, and it is given by

$$\overline{W}^{t^j}_{l+p,m+s} = \left(W^{j+1}_{l+p,m+s} - W^j_{l+p,m+s}\right)/\delta t, \quad p, s \in \{0, \pm 1\}. \tag{3.8}$$

The five-point single-cell compact scheme (3.7) is first-order exact along time axis and second-order accurate in xy-coordinate. Moreover, the magnitude of truncation error in the formula (3.7) remains unchanged with variably spaced meshes $\alpha \neq 0$ or $\beta \neq 0$, and uniformly spaced mesh points ($\alpha = \beta = 0$). Such a category of discretization has been classified as a supra-convergent scheme [25, 31]. The low order accurate scheme (3.7) lacks computational efficiency due to slow convergence, and may require many mesh points to achieve desired reliable numerical solutions. Thus, it is inevitable to design new numerical techniques that result in a more precise solution that needs a comparatively small number of mesh stencils. By enhancing the order of truncation error in a numerical scheme, one can receive solution values in comparatively short computing time with a faster convergence rate.

To develop a compact scheme of optimal accuracy, we start with time dependent PDEs.

$$\epsilon\nabla^2 W = \epsilon\left(\frac{\partial^2 W}{\partial x^2} + \frac{\partial^2 W}{\partial x^2}\right) = \psi(x, y, t). \tag{3.9}$$

At the mesh points (x_l, y_m, t_j), the PDEs (3.9) are expressed as

$$\epsilon\left(W^{xx^j}_{l,m} + W^{yy^j}_{l,m}\right) = \psi\left(x_l, y_m, t_j\right) \equiv \psi^j_{l,m}. \tag{3.10}$$

We consider the linear combination of ψ and its partial derivatives as

$$\chi \equiv \chi(x_l, y_m, t_j) = \delta x_l^2 \delta y_m^2 \Big[R_{00}\psi_{l,m}^j + R_{10}\delta x_l \psi_{l,m}^{x^j} + R_{01}\delta y_m \psi_{l,m}^{y^j} + R_{20}\delta x_l^2 \psi_{l,m}^{xx^j} + R_{02}\delta y_m^2 \psi_{l,m}^{yy^j} + R_{11}\delta x_l \delta y_m^2 \psi_{l,m}^{xy^j} \Big], \tag{3.11}$$

where R_{ns} are undetermined parameters to be obtained in such a way that it offer the high-order magnitude of local truncation error [26]. Applying the Taylor's series expansion to the compact operators (3.1)-(3.2) and its composites operaters on $\psi_{l,m}^j$ in the linear combination (3.11) and equating the higher-order terms to zero, we get

$$\begin{aligned} R_{10} &= \frac{\alpha}{3}\delta x_l R_{00}, \quad , R_{01} = \frac{\beta}{3}\delta y_m R_{00}, \quad R_{11} = \frac{\alpha\beta}{9}\delta x_l \delta y_m R_{00}, \\ R_{20} &= \frac{1}{12}(1+\alpha\delta x_l)R_{00}, \quad R_{02} = \frac{1}{12}(1+\beta\delta y_m)R_{00}. \end{aligned} \tag{3.12}$$

The survival of the linear combination (3.11) relies upon the choice of R_{00}. If $R_{00} = 0$, and the relation (3.11) collapses, we set R_{00} some non-zero finite value saying 1, and obtain

$$\chi = \epsilon \Big[\delta y_m^2 \mathcal{B}_x + \delta x_l^2 \mathcal{B}_y + \frac{1}{3}(\alpha\delta x_l^3 \mathcal{A}_x\mathcal{B}_y + \beta\delta y_m^3 \mathcal{A}_y\mathcal{B}_x) + R_{20}\delta x_l^2 \psi_{l,m}^{xx^j} + R_{02}\delta y_m^2 \psi_{l,m}^{yy^j} + R_{11}\delta x_l \delta y_m^2 \psi_{l,m}^{xy^j} \Big] \psi_{l,m}^j. \tag{3.13}$$

Moreover, by utilizing the compact operators expansion (3.5)-(3.6) on $\psi_{l,m}^j$, we substitute

$$\psi_{l,m}^{x^j} = \delta x_l^{-1}\mathcal{A}_x\psi_{l,m}^j, \quad \psi_{l,m}^{y^j} = \delta y_m^{-1}\mathcal{A}_y\psi_{l,m}^j, \tag{3.14}$$

$$\psi_{l,m}^{xx^j} = \delta x_l^{-2}\mathcal{B}_x\psi_{l,m}^j, \quad \psi_{l,m}^{yy^j} = \delta y_m^{-2}\mathcal{B}_y\psi_{l,m}^j, \psi_{l,m}^{xy^j} = \delta x_l^{-1}\delta y_m^{-2}\mathcal{A}_x\mathcal{A}_y\psi_{l,m}^j \tag{3.15}$$

in the relation (3.11) and equating it with (3.13), one obtains

$$\epsilon\overline{\nabla}^2 W_{l,m}^j = \delta x_l^2 \delta y_m^2 \left(\sum\nolimits_{(p,s)\in\mathcal{J}} \sigma_{l+p,m+s}\psi_{l+p,m+s} \right) + T_{l,m}^j, \tag{3.16}$$

where the summation runs over the set $\mathcal{J} = \{0, \pm 1\} \times \{0, \pm 1\}$, and

$$\overline{\nabla}^2 = \Big[\delta y_m^2 \mathcal{B}_x + \delta x_l^2 \mathcal{B}_y + \frac{1}{3}(\alpha\delta x_l^3 \mathcal{A}_x\mathcal{B}_y + \beta\delta y_m^3 \mathcal{A}_y\mathcal{B}_x) + \frac{1}{12}(\delta x_l \delta x_{l+1} + \delta y_m \delta y_{m+1})\mathcal{B}_x\mathcal{B}_y \Big] \psi_{l,m}^j, \tag{3.17}$$

is the high-order finite-difference discretization of Laplacian operator $\nabla^2 = \partial_{xx}^2 + \partial_{yy}^2$ and the expressions of coefficients $\sigma_{l+p,m+s}, (p,s) \in \mathcal{J}$ are presented in Appendix A. The truncation error associated with the scheme (3.17) is eight, and it is given by

$$T_{l,m}^j = O(\delta x_l^2 \delta y_m^2 \{\delta x_l^2 + \delta y_m^2\}^2) \tag{3.18}$$

for both zero and non-zero value of mesh expansion ratios α and β. Since the linear combination (3.11) begins with the multiple of fourth-order term $\delta x_l^2 \delta y_m^2$, the nine-point discretization discretization (3.16) must be divided into both sides by the same quantity to visualize the scheme-order: $\delta x_l^{-2}\delta y_m^{-2} T_{l,m}^j \approx O(\{\delta x_l^2 + \delta y_m^2\}^2)$. Consequently, we have obtained an optimal fourth-order accurate scheme to determine the numerical solution values of two-dimensional PDEs (3.9).

4. Two-level high-order implicit compact scheme

We will enhance the optimal order compact formulation (3.16) to the more general parabolic PDEs (1.3) that incorporate the unknown $W(x,y,t)$ and nonlinear interaction with its first-order partial derivatives. New discretization is based on two consecutive time levels and a convex combination of approximate solution values at nine-point stencils. Consider the following approximations

$$\bar{t}_j = (1-\rho)t_j + \rho t_{j+1}, \quad 0<\rho<1, \tag{4.1}$$

$$\overline{W}^{j}_{l+p,m+s} = (1-\rho)W^{j}_{l+p,m+s} + \rho W^{j+1}_{l+p,m+s}. \tag{4.2}$$

For $s=0,\pm 1$:

$$\begin{bmatrix} \overline{W}^{x^j}_{l+1,m+s} \\ \overline{W}^{x^j}_{l,m+s} \\ \overline{W}^{x^j}_{l-1,m+s} \end{bmatrix} = \frac{1}{\delta x_l}\mathcal{M}(\alpha,\delta x_l)\begin{bmatrix} \overline{W}^{j}_{l-1,m+s} \\ \overline{W}^{j}_{l,m+s} \\ \overline{W}^{j}_{l+1,m+s} \end{bmatrix},$$

$$\overline{W}^{xx^j}_{l,m+s} = \frac{2}{\delta x_l^2}\mathcal{N}(\alpha,\delta x_l)\begin{bmatrix} \overline{W}^{j}_{l-1,m+s} \\ \overline{W}^{j}_{l,m+s} \\ \overline{W}^{j}_{l+1,m+s} \end{bmatrix}. \tag{4.3}$$

For $p=0\pm 1$:

$$\begin{bmatrix} \overline{W}^{y^j}_{l+p,m+1} \\ \overline{W}^{y^j}_{l+p,m} \\ \overline{W}^{y^j}_{l+p,m-1} \end{bmatrix} = \frac{1}{\delta y_m}\mathcal{M}(\beta,\delta y_m)\begin{bmatrix} \overline{W}^{j}_{l+p,m-1} \\ \overline{W}^{j}_{l+p,m} \\ \overline{W}^{j}_{l+p,m+1} \end{bmatrix},$$

$$\overline{W}^{yy^j}_{l+p,m} = \frac{2}{\delta y_m^2}\mathcal{N}(\beta,\delta y_m)\begin{bmatrix} \overline{W}^{j}_{l+p,m-1} \\ \overline{W}^{j}_{l+p,m} \\ \overline{W}^{j}_{l+p,m+1} \end{bmatrix}, \tag{4.4}$$

where
$(\nu,h)\in\{(\alpha,\delta x_l),(\beta,\delta y_m)\}$, $\mathcal{N}(\nu,h)=\left[\frac{1}{2+\nu h}\ \frac{-1}{1+\nu h}\ \frac{1}{(1+\nu h)(2+\nu h)}\right]$ and

$$\mathcal{M}(\nu,h)=\begin{bmatrix} \frac{1+\nu h}{2+\nu h} & -\frac{2+\nu h}{1+\nu h} & \frac{3+2\nu h}{(1+\nu h)(2+\nu h)} \\ -\frac{1+\nu h}{2+\nu h} & \frac{\nu}{1+\nu h} & \frac{1}{(1+\nu h)(2+\nu h)} \\ -\frac{3+2\nu h}{2+\nu h} & \frac{2+\nu h}{1+\nu h} & -\frac{1}{(1+\nu h)(2+\nu h)} \end{bmatrix}.$$

By utilizing the approximations (4.1)-(4.4), we define the functional values for $(p,s)\in\overline{\mathcal{J}}=\mathcal{J}\sim\{(0,0)\}$ in the following manner

$$\overline{\psi}^{j}_{l+p,m+s} = \psi\left(x_{l+p}, y_{m+s}, \bar{t}_j, \overline{W}_{l+p,m+s}, \overline{W}^{x^j}_{l+p,m+s}, \overline{W}^{y^j}_{l+p,m+s}, \overline{W}^{t^j}_{l+p,m+s}\right). \tag{4.5}$$

Now, the updated approximations of convection terms at the central mesh location are defined by

$$\overline{\overline{W}}^{x^j}_{l,m} = \overline{W}^{x^j}_{l,m} + \gamma_x\delta x_l\left[\left(\overline{\psi}^{j}_{l+1,m} - \overline{\psi}^{j}_{l-1,m}\right) - \epsilon\left(\overline{W}^{yy^j}_{l+1,m} - \overline{W}^{yy^j}_{l-1,m}\right)\right] \tag{4.6}$$

and

$$\overline{\overline{W}}^{y^j}_{l,m} = \overline{W}^{y^j}_{l,m} + \gamma_y \delta y_m \left[\left(\overline{\psi}^j_{l,m+1} - \overline{\psi}^j_{l,m-1} \right) - \epsilon \left(\overline{W}^{xx^j}_{l,m+1} - \overline{W}^{yy^j}_{l,m-1} \right) \right]. \quad (4.7)$$

The undetermined parameters γ_x and γ_y in the approximations (4.6) and (4.7) are computed so as to yield the scheme of order two in time and order four in space. With the updated approximations of partial derivatives, we construct the functional at central mesh-point (x_l, y_m, t_j) as

$$\overline{\overline{\psi}}^j_{l,m} = \psi \left(x_l, y_m, \bar{t}_j, \overline{W}_{l,m}, \overline{\overline{W}}^{x^j}_{l,m}, \overline{\overline{W}}^{y^j}_{l,m}, \overline{W}^{t^j}_{l,m} \right). \quad (4.8)$$

Now, with the help of basic compact formulation (3.16), we obtain

$$\epsilon \overline{\nabla}^2 \overline{W}^j_{l,m} = \delta x_l^2 \delta y_m^2 \left(\sigma_{l,m} \overline{\overline{\psi}}^j_{l,m} + \sum\nolimits_{(p,s)\in\mathcal{J}} \sigma_{l+p,m+s} \overline{\psi}^j_{l,m} \right) + \overline{T}^j_{l,m}, \quad (4.9)$$

where the local truncation error $\overline{T}^j_{l,m}$ and truncation error T_E is computed as

$$\overline{T}^j_{l,m} = O(\delta x_l^2 \delta y_m^2 \{\delta x_l + \delta y_m\}^2 \delta t) \quad (4.10)$$

and

$$T_E = \delta x_l^{-2} \delta y_m^{-2} \overline{T}^j_{l,m} = O(\{\delta x_l + \delta y_m\}^2 \delta t), \quad (4.11)$$

provided

$$\gamma_x = -\frac{1 + \alpha \delta x_l}{8\epsilon(2 + \alpha \delta x_l)}, \;\; \gamma_y = -\frac{1 + \beta \delta y_m}{8\epsilon(2 + \beta \delta y_m)}, \;\; \text{and} \;\; \rho = \frac{1}{2}. \quad (4.12)$$

The numerical scheme (4.9) exhibits some unique properties: (i) It is compact and obtained with minimal meshes required to approximate the highest order differentials appeared in given parabolic PDEs; (ii) The compact formulation employs nine-point stencils with non-uniform mesh spacing; (iii) The truncation error is respectively second- and fourth-order in time and space. Moreover, it is practical to achieve fourth-order accurate numerical solution values, when $\delta t \propto \delta x_l^2 \approx \delta y_m^2$ or $\delta t \propto \delta x_l \delta y_m, \delta x_l \approx \delta y_m$ for all l and m; (iv) In either case, perhaps uniform or nonuniform dispersion of mesh points, the magnitude of truncation error remains unchanged; (v) The block tri-diagonal matrix structure of the scheme makes it easier to compute. For the computational purpose, we neglect the higher-order truncation term $T^j_{l,m}$ from the equation (4.9). By incorporating the initial and boundary data (1.4)-(1.6), the resulting well-structured system of difference equations (4.9) is solved by the Newton-Raphson method with suitable initial guess, when ψ is nonlinear. It is more advantageous to implement an alternating direction implicit method, when ψ is linear, and it is possible to obtain an operator splitting scheme.

5. Derivations of the high-order compact formulation

In this section, we present the derivation for the high-order scheme (4.9), and obtain high-order truncation error for the suitable choice of undetermined coefficients γ_x

and γ_y appearing in the updated approximations (4.6) and (4.7). By using Taylor's expansion to (4.2), we find

$$\overline{W}_{l,m}^{t^j} = W_{l,m}^{t^j} + \frac{1}{2}\delta t W_{l,m}^{tt^j} + \frac{1}{6}\delta t^2 W_{l,m}^{ttt^j} + O(\delta t^3), \tag{5.1}$$

$$\overline{W}_{l\pm1,m}^{t^j} = W_{l\pm1,m}^{t^j} + \frac{1}{2}\delta t\left[W_{l,m}^{tt^j} \pm \delta x_l W_{l,m}^{xtt^j}\right] + \frac{1}{6}\delta t^2 W_{l,m}^{ttt^j} + O(\delta x_l\{\delta x_l + \delta t\}\delta t), \tag{5.2}$$

$$\overline{W}_{l\pm1,m+1}^{t^j} = W_{l\pm1,m+1}^{t^j} + \frac{1}{2}\delta t\left[W_{l,m}^{tt^j} \pm \delta x_l W_{l,m}^{xtt^j} + \delta y_m W_{l,m}^{ytt^j}\right] + O(\delta t\{\delta x_l + \delta y_m\}^2 + \delta t^2), \tag{5.3}$$

$$\overline{W}_{l\pm1,m-1}^{t^j} = W_{l\pm1,m-1}^{t^j} + \frac{1}{2}\delta t\left[W_{l,m}^{tt^j} \pm \delta x_l W_{l,m}^{xtt^j} - \delta y_m W_{l,m}^{ytt^j}\right] + O(\delta t\{\delta x_l + \delta y_m\}^2 + \delta t^2), \tag{5.4}$$

$$\overline{W}_{l,m\pm1}^{t^j} = W_{l,m\pm1}^{t^j} + \frac{1}{2}\delta t\left[W_{l,m}^{tt^j} \pm \delta y_m W_{l,m}^{ytt^j}\right] + \frac{1}{6}\delta t^2 W_{l,m}^{ttt^j} + O(\delta y_m\{\delta x_l + \delta t\}\delta t). \tag{5.5}$$

Now, expanding (4.3)-(4.4), by Taylor's series, we obtain

$$\begin{bmatrix} \overline{W}_{l+1,m}^{x^j} \\ \overline{W}_{l,m}^{x^j} \\ \overline{W}_{l-1,m}^{x^j} \end{bmatrix} = \begin{bmatrix} W_{l+1,m}^{x^j} \\ W_{l,m}^{x^j} \\ W_{l-1,m}^{x^j} \end{bmatrix} + P_x Q_x + T, \tag{5.6}$$

$$\begin{bmatrix} \overline{W}_{l+1,m\pm1}^{x^j} \\ \overline{W}_{l,m\pm1}^{x^j} \\ \overline{W}_{l-1,m\pm1}^{x^j} \end{bmatrix} = \begin{bmatrix} W_{l+1,m\pm1}^{x^j} \\ W_{l,m\pm1}^{x^j} \\ W_{l-1,m\pm1}^{x^j} \end{bmatrix} + P_x Q_x \pm S R_x + T, \tag{5.7}$$

$$\begin{bmatrix} \overline{W}_{l,m+1}^{y^j} \\ \overline{W}_{l,m+1}^{y^j} \\ \overline{W}_{l,m+1}^{y^j} \end{bmatrix} = \begin{bmatrix} W_{l,m+1}^{y^j} \\ W_{l,m}^{y^j} \\ W_{l,m-1}^{y^j} \end{bmatrix} + P_y Q_y + T, \tag{5.8}$$

$$\begin{bmatrix} \overline{W}_{l\pm1,m+1}^{y^j} \\ \overline{W}_{l\pm1,m}^{y^j} \\ \overline{W}_{l\pm1,m-1}^{y^j} \end{bmatrix} = \begin{bmatrix} W_{l\pm1,m+1}^{y^j} \\ W_{l\pm1,m}^{y^j} \\ W_{l\pm1,m-11}^{y^j} \end{bmatrix} + P_y Q_y \pm S R_y + T, \tag{5.9}$$

where

$$P_x = \begin{bmatrix} 1 - \dfrac{\delta x_l^2(2+3\alpha\delta x_l)}{6} & 1 & -\dfrac{1}{12} \\ 1 & \dfrac{\delta x_l^2(2+3\alpha\delta x_l)}{6} & 0 \quad 0 \\ 1 - \dfrac{\delta x_l^2(2+3\alpha\delta x_l)}{6} & -1 & \dfrac{1}{12} \end{bmatrix}, P_y = \begin{bmatrix} 1 - \dfrac{\delta y_m^2(2+3\beta\delta y_m)}{6} & 1 & -\dfrac{1}{12} \\ 1 & \dfrac{\delta y_m^2(2+3\beta\delta y_m)}{6} & 0 \quad 0 \\ 1 - \dfrac{\delta y_m^2(2+3\beta\delta y_m)}{6} & -1 & \dfrac{1}{12} \end{bmatrix}$$

$$Q_x = \begin{bmatrix} \rho\delta t W_{l,m}^{xt^j} \\ W_{l,m}^{xxx^j} \\ \rho\delta t\delta x_l W_{l,m}^{xxt^j} \\ \delta x_l^3 W_{l,m}^{xxxx^j} \end{bmatrix}, \qquad Q_y = \begin{bmatrix} \rho\delta t W_{l,m}^{yt^j} \\ W_{l,m}^{yyy^j} \\ \rho\delta t\delta y_m W_{l,m}^{yyt^j} \\ \delta y_m^3 W_{l,m}^{yyyy^j} \end{bmatrix},$$

$$R_x = \begin{bmatrix} \rho\delta t\delta y_m W_{l,m}^{xyt^j} \\ \delta x_l^2 \delta y_m W_{l,m}^{xxxy^j} \end{bmatrix}, \qquad R_y = \begin{bmatrix} \rho\delta t\delta x_l W_{l,m}^{xyt^j} \\ \delta x_l^2 \delta x_l W_{l,m}^{xyyy^j} \end{bmatrix}$$

and

$$S = \begin{bmatrix} 6 & -2 \\ 6 & 1 \\ 6 & -2 \end{bmatrix}, \qquad T = \begin{bmatrix} O(\delta t(\delta x_l + \delta y_m)^2 + \delta t^2) \\ O(\delta t(\delta x_l + \delta y_m)^2 + \delta t^2) \\ O(\delta t(\delta x_l + \delta y_m)^2 + \delta t^2) \end{bmatrix}.$$

The functional approximations (4.5) at the mesh locations $x_{l+p,m+s}, (p,s) \in \overline{\mathcal{J}}$, in combination with (5.1)-(5.9), are computed as

$$\begin{aligned} \begin{bmatrix} \overline{\psi}_{l-1,m\pm1}^j \\ \overline{\psi}_{l,m\pm1}^j \\ \overline{\psi}_{l+1,m\pm1}^j \end{bmatrix} &= \begin{bmatrix} \psi_{l-1,m\pm1}^j \\ \psi_{l,m\pm1}^j \\ \psi_{l+1,m\pm1}^j \end{bmatrix} + Z_1 S_1^{\pm1} + Z_2 S_2^{\pm1} \\ &\quad + Z_3 S_3^{\pm1} + Z_4 S_4^{\pm1} + bf Z_5 S_5^{\pm1} + Z_6 S_6^{\pm1}, \end{aligned} \tag{5.10}$$

$$\begin{aligned} \begin{bmatrix} \overline{\psi}_{l-1,m}^j \\ \overline{\psi}_{l,m}^j \\ \overline{\psi}_{l+1,m}^j \end{bmatrix} &= \begin{bmatrix} \psi_{l-1,m}^j \\ \psi_{l,m}^j \\ \psi_{l+1,m}^j \end{bmatrix} + S_1^0 Z_1^0 + S_2^0 Z_2^0 \\ &\quad + S_3^0 Z_3^0 + S_4^0 Z_4^0 + S_5^0 Z_5^0 + S_5^0 Z_5^0, \end{aligned} \tag{5.11}$$

where the expression of matrices $S_i^0, i = 1(1)5, S_k^{\pm1}$ and vectors $Z_s, s = 1(1)6, k = 1(1)5$ are presented in Appendix B. By using (4.3), (4.4), (5.10) and (5.11) in (4.6)-(4.7), we find that

$$\begin{aligned} \overline{\overline{W}}_{l,m}^{x^j} = W_{l,m}^{x^j} + \rho\delta t W_{l,m}^{xt^j} + \frac{\delta x_l^2}{6}\left[1 + 12\epsilon\gamma_x + \alpha(1 + 6\epsilon\gamma_x)\delta x_l\right] W_{l,m}^{xxx^j} \\ + O(\delta t(\delta x_l + \delta y_m)^2 + \delta t^2), \end{aligned} \tag{5.12}$$

$$\begin{aligned} \overline{\overline{W}}_{l,m}^{y^j} = W_{l,m}^{y^j} + \rho\delta t W_{l,m}^{yt^j} + \frac{\delta y_m^2}{6}\left[1 + 12\epsilon\gamma_y + \beta(1 + 6\epsilon\gamma_y)\delta y_m\right] W_{l,m}^{yyy^j} \\ + O(\delta t(\delta x_l + \delta y_m)^2 + \delta t^2). \end{aligned} \tag{5.13}$$

Therefore, the functional approximation at the central mesh-point by utilizing (5.12) and (5.13), in updated functional (4.8), one finds

$$\begin{aligned} \overline{\overline{\psi}}_{l,m}^j = &\psi_{l,m}^j + \rho\delta t\left(A + BW_{l,m}^{t^j} + CW_{l,m}^{xt^j} + DW_{l,m}^{yt^j}\right) + \frac{1}{2}E\delta t W_{l,m}^{tt^j} \\ &+ \frac{1}{6}\delta x_l^2\left[1 + 12\epsilon\gamma_x + \alpha(1 + 6\epsilon\gamma_x)\delta x_l\right] CW_{l,m}^{xxx^j} \\ &+ \frac{1}{6}\delta y_m^2\left[1 + 12\epsilon\gamma_y + \alpha(1 + 6\epsilon\gamma_y)\delta y_m\right] DW_{l,m}^{yyy^j} \\ &+ O(\delta t(\delta x_l + \delta y_m)^2 + \delta t^2). \end{aligned} \tag{5.14}$$

Upon differentiating the nonlinear parabolic PDEs (1.3) with respect to t and their evaluation at the mesh-point (x_l, y_m, t_j) gives

$$\epsilon\left(W_{l,m}^{xxt^j} + W_{l,m}^{yyt^j}\right) = A + BW_{l,m}^{t^j} + CW_{l,m}^{xt^j} + DW_{l,m}^{yt^j} + EW_{l,m}^{tt^j}, \tag{5.15}$$

where $A = \dfrac{\partial \psi}{\partial t}, B = \dfrac{\partial \psi}{\partial W}, C = \dfrac{\partial \psi}{\partial W^x}, D = \dfrac{\partial \psi}{\partial W^y}$ are values evaluated at the mesh-point (x_l, y_m, t_j). Notations A_x, A_y, etc. are adopted to denote the partial derivatives of A with respect to x and y respectively at the mesh location (x_l, y_m, t_j). Now, substituting (5.10), (5.11),(5.14) in (4.9) and utilizing (5.15), we obtain

$$\begin{aligned}\epsilon\overline{\overline{\nabla}}^2\overline{W}^j_{l,m} - \delta x_l^2\delta y_m^2\left(\sigma_{l,m}\overline{\overline{\psi}}^j_{l,m} + \sum\nolimits_{(p,s)\in\overline{\mathcal{J}}}\sigma_{l+p,m+s}\overline{\psi}^j_{l,m}\right)\\ = \frac{1}{12}\delta x_l^4\delta y_m^2\left[1+\alpha\delta x_l + 8\epsilon\gamma_x(\alpha\delta x_l+2)\right]CW^{xxx^j}_{l,m}\\ + \frac{1}{12}\delta y_m^4\delta x_l^2\left[1+\beta\delta y_m + 8\epsilon\gamma_y(\beta\delta y_m+2)\right]DW^{yyy^j}_{l,m}\\ + \frac{1}{2}\delta x_l^2\delta y_m^2\delta t(1-2\rho)EW^{tt^j}_{l,m} + \overline{T}^j_{l,m}. \end{aligned} \tag{5.16}$$

The coefficients of $W^{xxx^j}_{l,m}, W^{yyy^j}_{l,m}, W^{tt^j}_{l,m}$, appearing in the equation (5.16), vanish for the values of γ_x, γ_y and ρ mentioned in (4.12). Consequently, the resulting difference scheme (4.9) supplies an accuracy of order four in xy-space and order two along time axis.

6. Convection-diffusion equation and implement alternating direction implicit (ADI) scheme

The class of 2D convection-diffusion equations has been considered across-the-board to model many physical phenomena such as nuclear waste disposal, pattern formation and mobility of fish population [29,48]. We will formulate the operator splitting scheme and implement alternating direction implicit (ADI) method for the solution of two-dimensions convection dominated diffusion equation

$$\epsilon\left(\frac{\partial^2 W}{\partial x^2} + \frac{\partial^2 W}{\partial y^2}\right) = \frac{\partial W}{\partial t} + a\frac{\partial W}{\partial x} + c\frac{\partial W}{\partial t} + g(x,y,t), \tag{6.1}$$

along with boundary and initial data (1.4)-(1.6). Here, a and b are constants, and $W(x,y,t)$ is the concentration of heat transfer. Upon substituting

$$\overline{\psi}^j_{l+p,m+s} = \overline{W}^{t^j}_{l+p,m+s} + a\overline{W}^{x^j}_{l+p,m+s} + b\overline{W}^{y^j}_{l+p,m+s} + \overline{g}^j_{l+p,m+s}, (p,s)\in\overline{\mathcal{J}}, \tag{6.2}$$

$$\overline{\overline{\psi}}^j_{l,m} = \overline{W}^{t^j}_{l,m} + a\overline{\overline{W}}^{x^j}_{l,m} + b\overline{\overline{W}}^{y^j}_{l,m} + \overline{g}^j_{l,m}, \tag{6.3}$$

$$\overline{g}^j_{l+p,m+s} = g(x_{l+p}, y_{m+s}, \bar{t}_j), (p,s)\in\mathcal{J}. \tag{6.4}$$

in the compact formulation (4.9), we obtain a system of difference equations

$$\begin{aligned}\overline{\nabla}^2 =& \delta x_l^2\delta y_m^2\Big[\sum\nolimits_{(p,s)\in\mathcal{J}}\sigma_{l+p,m+s}\left(\overline{W}^{t^j}_{l+p,m+s} + \overline{g}_{l+p,m+s}\right)\\ &+ \sum\nolimits_{(p,s)\in\overline{\mathcal{J}}}\sigma_{l+p,m+s}\left(a\overline{W}^{x^j}_{l+p,m+s} + b\overline{W}^{y^j}_{l+p,m+s}\right)\\ &+ \sigma_{l,m}\left(a\overline{\overline{W}}^{x^j}_{l,m} + b\overline{\overline{W}}^{y^j}_{l,m}\right)\Big] + \overline{T}^j_{l,m}. \end{aligned} \tag{6.5}$$

The system of difference equations (4.9) yields a large sparse matrix system, and its solution procedure is quite a time consuming due to a large number of time levels, and each time level carry $(L+2)(M+2)$ spatial mesh points. Moreover, most of the memory locations are occupied with zero value. Thus, we intend to develop operator splitting pattern as an efficient memory management technique. To do so, at j^{th} and $(j+1)^{th}$ time levels, we express the solution values $W^j_{l+p,m+s}, W^{j+1}_{l+p,m+s}, (p,s) \in \overline{\mathcal{J}}$, at eight neighborhood points of the central mesh-point (x_l, y_m, t_j) in terms of the compact operators (3.1)-(3.2) and their composites. For example, the operator equation in (3.1) can be solved jointly to obtain

$$W^j_{l+1,m} = \frac{1}{2}\left[2 + (1+\alpha\delta x_l)\left\{(1+\alpha\delta x_l)\mathcal{B}_x + \mathcal{A}_x\right\}\right] W^j_{l,m}, \tag{6.6}$$

$$W^j_{l-1,m} = \frac{1}{2}\left[2 - 2\mathcal{A}_x + \mathcal{B}_x\right] W^j_{l,m}. \tag{6.7}$$

Similarly, it is feasible to express solution values at other mesh locations (except at central mesh-point) by using compact operators (3.2) and their composites. The solution values at $(j+1)^{th}$ -time level is determined by interchanging j to $j+1$ in the above relations (6.6) and (6.7). Such a replacement of solution values in terms of operators to the difference equation (6.5) and dividing throughout by $\delta x_l \delta y_m$, one obtains

$$\mathcal{L} W^{j+1}_{l,m} = \mathcal{R} W^j_{l,m} + \sum\nolimits_{RHS} + \overline{\overline{T}}^j_{l,m}, \tag{6.8}$$

where the left and right side operators are

$$\begin{aligned}\mathcal{L} =& 1 + P_1\mathcal{A}_x + P_2\mathcal{B}_x + P_3\mathcal{A}_y + P_4\mathcal{B}_y \\ &+ P_5\mathcal{A}_x\mathcal{B}_y + P_6\mathcal{B}_x\mathcal{A}_y + P_7\mathcal{A}_x\mathcal{A}_y + P_8\mathcal{B}_x\mathcal{B}_y, \end{aligned}\tag{6.9}$$

$$\begin{aligned}\mathcal{R} =& 1 + Q_1\mathcal{A}_x + Q_2\mathcal{B}_x + Q_3\mathcal{A}_y + Q_4\mathcal{B}_y \\ &+ Q_5\mathcal{A}_x\mathcal{B}_y + Q_6\mathcal{B}_x\mathcal{A}_y + Q_7\mathcal{A}_x\mathcal{A}_y + Q_8\mathcal{B}_x\mathcal{B}_y, \end{aligned}\tag{6.10}$$

$$\begin{aligned}&\sum\nolimits_{RHS} = \sum\nolimits_{(p,q)\in\mathcal{J}} R_{l+p,m+q}\overline{g}^j_{l+p,m+q}, \\ &\overline{\overline{T}}^j_{l,m} = \delta x_l^{-1}\delta y_m^{-1}\overline{T}^j_{l,m} = O(\delta x_l \delta y_m(\delta x_l + \delta y_m)^2\delta t). \end{aligned}\tag{6.11}$$

The values of $P_i, Q_i, i = 1(1)8$ and $R_{l+p,m+s}, (p,s) \in \mathcal{J}$ are listed in Appendix C. We shall reframe the linear system (6.8) in operator splitting form that results in efficient space-time mechanism.
Let

$$\widehat{\mathcal{L}} = \left(1 + P_1\mathcal{A}_x + P_2\mathcal{B}_x\right)\left(1 + P_3\mathcal{A}_y + P_4\mathcal{B}_y\right), \tag{6.12}$$

$$\widehat{\mathcal{R}} = \left(1 + Q_1\mathcal{A}_x + Q_2\mathcal{B}_x\right)\left(1 + Q_3\mathcal{A}_y + Q_4\mathcal{B}_y\right). \tag{6.13}$$

By using (6.9), (6.10), (6.12) and (6.13), we obtain

$$\left(\widehat{\mathcal{L}} - \mathcal{L} - \chi^+\right) W^{j+1}_{l,m} = 0 \ \text{ and } \ \left(\widehat{\mathcal{R}} - \mathcal{R} + \chi^-\right) W^j_{l,m} = 0, \tag{6.14}$$

where the residual operators $\chi^{\pm}$, left after the factorization are given by

$$\chi^+ = E_1\mathcal{B}_x\mathcal{B}_y + E_2\mathcal{B}_x\mathcal{A}_y + E_3\mathcal{A}_x\mathcal{B}_y + E_4\mathcal{A}_x\mathcal{A}_y, \tag{6.15}$$

$$\chi^+ = F_1\mathcal{B}_x\mathcal{B}_y + F_2\mathcal{B}_x\mathcal{A}_y + F_3\mathcal{A}_x\mathcal{B}_y + F_4\mathcal{A}_x\mathcal{A}_y, \tag{6.16}$$
$$E_1 = P_2P_4 - P_8, E_2 = P_2P_3 - P_6, E_3 = P_1P_4 - P_5, E_4 = P_1P_3 - P_7,$$
$$F_1 = Q_8 - Q_2Q_4, F_2 = Q_6 - Q_2Q_3, F_3 = Q_5 - Q_1Q_4, F_4 = Q_7 - Q_1Q_3.$$

As a result, the difference scheme (6.8) can be rewritten as

$$\widehat{\mathcal{L}}W_{l,m}^{j+1} = \widehat{\mathcal{R}}W_{l,m}^{j} + \chi^+W_{l,m}^{j+1} + \chi^-W_{l,m}^{j+1} + \sum\nolimits_{RHS} + \overline{\overline{T}}_{l,m}^{j}. \tag{6.17}$$

The application of Taylor's series expansion on $E_i, F_i, i = 1(1)4$, and making use of the approximations $W_{l,m}^{j+1} = W_{l,m}^{j} + O(\delta t)$, one finds that

$$\chi^+W_{l,m}^{j+1} + \chi^-W_{l,m}^{j} = O(\delta t(\delta x_l^2 + \delta y_m^2)^2). \tag{6.18}$$

As a consequence, the scheme (6.17) further simplifies to the compact operator splitting form as

$$\overline{\mathcal{L}}W_{l,m}^{j+1} = \overline{\mathcal{R}}W_{l,m}^{j} + \sum\nolimits_{RHS} + \widehat{T}_{l,m}^{j}, \tag{6.19}$$

where

$$\widehat{T}_{l,m}^{j} = \overline{\overline{T}}_{l,m}^{j} + O(\delta t(\delta x_l^2 + \delta y_m^2)^2) \approx O(\{\delta x_l + \delta y_m\}^4)\delta t). \tag{6.20}$$

Upon neglecting higher-order terms $\widehat{T}_{l,m}^{j}$ from the operator splitting scheme (6.19), we shall easily implement the alternating direction implicit method in the following manner

$$\left(1 + P_1\mathcal{A}_y + P_2\mathcal{B}_y\right)W_{l,m}^{j+1/2} = \chi^-W_{l,m}^{j} + \sum\nolimits_{RHS}, \tag{6.21}$$
$$\left(1 + P_1\mathcal{A}_x + P_2\mathcal{B}_x\right)W_{l,m}^{j} = W_{l,m}^{j+1/2}. \tag{6.22}$$

Here, $W_{l,m}^{j+1/2}$ is an intermediary step, appearing in the middle of j^{th} and $(j+1)^{th}$ temporal level, and one may determine intermediate boundary data from (6.21) in combination with available initial and boundary values (1.4)-(1.6).

Computationally, the number of mesh points along time and spatial directions are chosen, so that $\delta t \propto \delta x_l\delta y_m$ and $\delta y_m \propto \delta x_l$. This makes the magnitude of local truncation errors $\overline{\overline{T}}_{l,m}^{j}$ and $\widehat{T}_{l,m}^{j}$ in the non-factored scheme (6.8) and operator splitting scheme (6.19) respectively in a comparable order. Apart from it, we have factored the scheme (6.8), keeping in view that the maximum magnitude of discretization error appears from the term $\mathcal{B}_x\mathcal{B}_y$, (coefficient of P_8). This is because $\mathcal{B}_x\mathcal{B}_yW_{l,m}^{j+1} = \mathcal{B}_x\mathcal{B}_y\left(W_{l,m}^{j} + O(\delta t)\right)$ that provides discretization error $O(\delta t\delta x_l^2\delta y_m^2)$, and the temporal step choice $\delta t \propto \delta x_l\delta y_m$ left us with an error of $O(\delta x_l^3\delta y_m^3)$, almost sixth-order local truncation error. This is one of the main issues encountered in the operator splitting procedure. Hence, it is necessary to divide throughout the scheme (6.5) by $\delta x_l\delta y_m$ to bring down the local truncation error from $\overline{T}_{l,m}^{j}$ to $\overline{\overline{T}}_{l,m}^{j}$. Moreover, the magnitude of local truncation errors $\overline{\overline{T}}_{l,m}^{j}$ in the non-factored scheme (6.8) and $\widehat{T}_{l,m}^{j}$ in the operator splitting scheme (6.19) is comparable to the sixth-order local truncation error. Therefore, we can conclude that the two-level implicit operator splitting scheme (6.19) provides fourth-order accurate solution values for $\delta t \propto \delta x_l\delta y_m$, and the factored compact formulations (6.21) and (6.22) can be solved using the tri-diagonal solver (Thomas algorithm) efficiently.

7. Coupled Burger's equation and stability theory

Burger's equation appears in the weak non-stationary shock wave and modeling of turbulence. An analytic solution to one-dimensional Burger's equation was initially described by Cole [7]. An extension to the coupled form of Burger's equation to model the polydispersive sedimentation was proposed by Esipov [11]. The two-dimensions Burger's equations are the same as the Navier-Stokes equation in the absence of pressure gradient, and its analytic solution was reported in [13,45]. The two dimensions Burger's equations are

$$\epsilon\left(\frac{\partial^2 U}{\partial x^2}+\frac{\partial^2 U}{\partial y^2}\right)=\frac{\partial U}{\partial t}+U\frac{\partial U}{\partial x}+V\frac{\partial U}{\partial y}, \tag{7.1}$$

$$\epsilon\left(\frac{\partial^2 V}{\partial x^2}+\frac{\partial^2 V}{\partial y^2}\right)=\frac{\partial V}{\partial t}+U\frac{\partial V}{\partial x}+V\frac{\partial V}{\partial y}, \tag{7.2}$$

where $U=U(x,y,t), V=V(x,y,t)$, are velocity components, $Re=1/\epsilon$ denotes Reynolds number used to predict the pattern of fluid flow [22]. One can extend the high-order quasi-variable mesh compact scheme (4.9) to discretize the coupled PDEs (7.1) and (7.2) in the following manner:

$$\overline{\overline{F}}^{j}_{l+p,m+s}=\overline{U}^{t^j}_{l+p,m+s}+\overline{U}^{j}_{l+p,m+s}\overline{U}^{x^j}_{l+p,m+s}+\overline{V}^{j}_{l+p,m+s}\overline{U}^{y^j}_{l+p,m+s}, \tag{7.3}$$

$$\overline{\overline{F}}^{j}_{l+p,m+s}=\overline{U}^{t^j}_{l+p,m+s}+\overline{U}^{j}_{l+p,m+s}\overline{U}^{x^j}_{l+p,m+s}+\overline{V}^{j}_{l+p,m+s}\overline{U}^{y^j}_{l+p,m+s}, (p,s)\in\overline{\mathcal{J}}, \tag{7.4}$$

$$\overline{U}^{xx^j}_{l,m\pm s}=\frac{2}{\delta x_l^2}\mathcal{N}(\alpha,\delta x_l)\begin{bmatrix}\overline{U}^{j}_{l-1,m\pm s}\\ \overline{U}^{j}_{l,m\pm s}\\ \overline{U}^{j}_{l+1,m\pm s}\end{bmatrix}, s=0,1,$$

$$\overline{V}^{xx^j}_{l,m\pm s}=\frac{2}{\delta x_l^2}\mathcal{N}(\alpha,\delta x_l)\begin{bmatrix}\overline{V}^{j}_{l-1,m\pm s}\\ \overline{V}^{j}_{l,m\pm s}\\ \overline{V}^{j}_{l+1,m\pm s}\end{bmatrix}, s=0,1, \tag{7.5}$$

$$\overline{U}^{yy^j}_{l\pm p,m}=\frac{2}{\delta y_m^2}\mathcal{N}(\beta,\delta y_m)\begin{bmatrix}\overline{U}^{j}_{l\pm p,m-1}\\ \overline{U}^{j}_{l\pm p,m}\\ \overline{U}^{j}_{l\pm p,m+1}\end{bmatrix}, p=0,1,$$

$$\overline{V}^{yy^j}_{l\pm p,m}=\frac{2}{\delta y_m^2}\mathcal{N}(\beta,\delta y_m)\begin{bmatrix}\overline{V}^{j}_{l\pm p,m-1}\\ \overline{V}^{j}_{l\pm p,m}\\ \overline{V}^{j}_{l\pm p,m+1}\end{bmatrix}, p=0,1, \tag{7.6}$$

The weighted average $\overline{U}^{j}_{l+p,m+s}, \overline{V}^{j}_{l+p,m+s}, (p,s)\in\mathcal{J}$ and approximations of first-order partial derivatives of $U(x,y,t)$, and $V(x,y,t)$, at various mesh locations are obtained from (4.2)-(4.4) by interchanging W to U and V respectively. The updated partial derivatives at the central mesh-point (x_l,y_m,t_j) can be extended as

$$\overline{\overline{U}}^{x^j}_{l,m}=\overline{U}^{x^j}_{l,m}+\gamma_x\delta x_l\left[\overline{F}^{j}_{l+1,m}-\overline{F}^{j}_{l-1,m}-\epsilon\left(\overline{U}^{yy^j}_{l+1,m}-\overline{U}^{yy^j}_{l-1,m}\right)\right], \tag{7.7}$$

$$\overline{\overline{U}}^{y^j}_{l,m} = \overline{U}^{y^j}_{l,m} + \gamma_y \delta y_m \left[\overline{F}^j_{l+1,m} - \overline{F}^j_{l-1,m} - \epsilon \left(\overline{U}^{xx^j}_{l,m+1} - \overline{U}^{xx^j}_{l,m-1} \right) \right], \tag{7.8}$$

$$\overline{\overline{V}}^{x^j}_{l,m} = \overline{V}^{x^j}_{l,m} + \gamma_x \delta x_l \left[\overline{G}^j_{l+1,m} - \overline{G}^j_{l-1,m} - \epsilon \left(\overline{V}^{yy^j}_{l+1,m} - \overline{V}^{yy^j}_{l-1,m} \right) \right], \tag{7.9}$$

$$\overline{\overline{V}}^{y^j}_{l,m} = \overline{V}^{y^j}_{l,m} + \gamma_y \delta y_m \left[\overline{G}^j_{l+1,m} - \overline{G}^j_{l-1,m} - \epsilon \left(\overline{V}^{xx^j}_{l,m+1} - \overline{V}^{xx^j}_{l,m-1} \right) \right]. \tag{7.10}$$

Here, γ_x and γ_y are same as obtained in (4.12). Now, the updated functional values at the central mesh-point (x_l, y_m, t_j) are obtained as

$$\overline{\overline{F}}^j_{l,m} = \overline{U}^{t^j}_{l,m} + \overline{U}^j_{l,m} \overline{\overline{U}}^{x^j}_{l,m} + \overline{V}^j_{l,m} \overline{\overline{U}}^{y^j}_{l,m}, \tag{7.11}$$

$$\overline{\overline{G}}^j_{l,m} = \overline{V}^{t^j}_{l,m} + \overline{U}^j_{l,m} \overline{\overline{V}}^{x^j}_{l,m} + \overline{V}^j_{l,m} \overline{\overline{V}}^{y^j}_{l,m}. \tag{7.12}$$

Therefore, the nine-point high-order compact discretization using quasi-variable meshes network for solving the coupled Burger's equation (7.1) and (7.2) is given by

$$\overline{T}^{(U)} = \epsilon \overline{\nabla}^2 U^j_{l,m} + \left[\sigma_{l,m} \overline{\overline{F}}^j_{l,m} + \sum\nolimits_{(p,s)\in\overline{\mathcal{J}}} \sigma_{l+p,m+s} \overline{F}^j_{l,m} \right], \tag{7.13}$$

$$\overline{T}^{(V)} = \epsilon \overline{\nabla}^2 V^j_{l,m} + \left[\sigma_{l,m} \overline{\overline{G}}^j_{l,m} + \sum\nolimits_{(p,s)\in\overline{\mathcal{J}}} \sigma_{l+p,m+s} \overline{G}^j_{l,m} \right]. \tag{7.14}$$

The solution values in the succeeding temporal level for the system of nonlinear difference equation (7.13) and (7.14) is determined by applying the Newton-Raphson method

$$\begin{bmatrix} U^{j+1}_{l,m} \\ V^{j+1}_{l,m} \end{bmatrix} = \begin{bmatrix} U^j_{l,m} \\ V^j_{l,m} \end{bmatrix} - \mathcal{J}^{-1} \begin{bmatrix} T^{(U)} \\ T^{(V)} \end{bmatrix}, \mathcal{J} = \begin{bmatrix} \dfrac{\partial T^{(U)}}{\partial U^j_{l,m}} & \dfrac{\partial T^{(U)}}{\partial V^j_{l,m}} \\ \dfrac{\partial T^{(V)}}{\partial U^j_{l,m}} & \dfrac{\partial T^{(V)}}{\partial V^j_{l,m}} \end{bmatrix} \tag{7.15}$$

with $\mathcal{J}$ being the Jacobian of iteration matrix.

We shall describe the Hopf-Cole transformation to the coupled Burger's equation (7.1)-(7.2), assuming $[U, V]$ is irrotational. Let $[U, V] = \nabla\mathcal{F}$, and integrating (7.1)-(7.2) with respect to x and y, one obtains

$$\epsilon \left(\frac{\partial^2 \mathcal{F}}{\partial x^2} + \frac{\partial^2 \mathcal{F}}{\partial y^2} \right) = \frac{\partial \mathcal{F}}{\partial t} + \frac{1}{2} \left[\left(\frac{\partial \mathcal{F}}{\partial x} \right)^2 + \left(\frac{\partial \mathcal{F}}{\partial y} \right)^2 \right] + C(t), \tag{7.16}$$

A further substitution $\mathcal{F} = -2\epsilon \ln(H(x, y, t))$ to the equation (7.16) results in

$$\epsilon \left(\frac{\partial^2 H}{\partial x^2} + \frac{\partial^2 H}{\partial y^2} \right) = \frac{\partial H}{\partial t} - \frac{H}{2\epsilon} C(t). \tag{7.17}$$

Finally, the substitution $H(x, y, t) = E(t)W(x, y, t)$, $E(t) = e^{\frac{1}{2}\int C(t)dt}$ transforms the equation (7.17) to the two-dimensional pure diffusion equation

$$\epsilon \left(\frac{\partial^2 W}{\partial x^2} + \frac{\partial^2 W}{\partial y^2} \right) = \frac{\partial W}{\partial t}. \tag{7.18}$$

Next, we shall describe the stability theory of the alternating direction implicit compact scheme for the standard diffusion equation (7.18). The operator splitting scheme to the equation (7.18) can be obtained from (6.21)-(6.22) by substituting $a = 0, b = 0$ and setting source function $g(x, y, t)$ as zero. Following the technique described in [35, 46], we take $\epsilon_{l,m}^{j} = \xi^{j} e^{i(\eta x_l + \tau y_m)}$ as the error at j^{th}-time level, where ξ is an amplification factor, a complex constant, η and τ are real numbers, and $i = \sqrt{-1}$. Thus, the error equation is given by

$$\begin{aligned}(1 + P_1\mathcal{A}_x + P_2\mathcal{B}_x)\,(1 + P_3\mathcal{A}_y + P_4\mathcal{B}_y)\,\epsilon_{l,m}^{j+1} = \\ (1 + P_1\mathcal{A}_x + P_2\mathcal{B}_x)\,(1 + P_3\mathcal{A}_y + P_4\mathcal{B}_y)\,\epsilon_{l,m}^{j}.\end{aligned} \tag{7.19}$$

Since $\epsilon_{l,m}^{j+1} = \xi\epsilon_{l,m}^{j}, x_{l+1} = x_l + \delta x_{l+1}, x_{l-1} = x_l - \delta x_l, y_{m+1} = y_m + \delta y_{m+1}$ and $y_{m-1} = y_m - \delta y_m$. Thus, from the relations (3.1), (3.2), we obtain

$$\begin{bmatrix}\mathcal{A}_x \\ \mathcal{B}_x\end{bmatrix}\epsilon_{l,m}^{j+1} = \xi_x \begin{bmatrix}\mathcal{A}_x \\ \mathcal{B}_x\end{bmatrix}\epsilon_{l,m}^{j}, \qquad \begin{bmatrix}\mathcal{A}_y \\ \mathcal{B}_y\end{bmatrix}\epsilon_{l,m}^{j+1} = \xi_y \begin{bmatrix}\mathcal{A}_y \\ \mathcal{B}_y\end{bmatrix}\epsilon_{l,m}^{j} \quad . \tag{7.20}$$

Therefore, the amplification factor is obtained as $\xi = \xi_x\xi_y$, where

$$\begin{bmatrix}\xi_x \\ \xi_y\end{bmatrix} = \begin{bmatrix}N_x/D_x \\ N_y/D_y\end{bmatrix} = \begin{bmatrix}(1 + Q_1\mathcal{A}_x + Q_2\mathcal{B}_x)\,/\,(1 + P_1\mathcal{A}_x + P_2\mathcal{B}_x) \\ (1 + Q_3\mathcal{A}_y + Q_4\mathcal{B}_y)\,/\,(1 + P_3\mathcal{A}_y + P_4\mathcal{B}_y)\end{bmatrix}. \tag{7.21}$$

If we denote $L_x = (N_x - D_x)\,/\,(N_x + D_x)$ and $L_y = (N_y - D_y)\,/\,(N_y + D_y)$, then one can express

$$\xi_x = [1 + L_x]/[1 - L_x], L_x = [\widetilde{A}_x + i\widetilde{B}_x]/[\widetilde{C}_x + i\widetilde{D}_x], \tag{7.22}$$

where

$$\begin{aligned}\widetilde{A}_x =& 192\epsilon\lambda_{l,m}\delta x_l\delta_m(1 + \beta\delta y_m)(2 + \beta\delta y_m) \\ & \{\beta\delta y_m - (1 + \beta\delta y_m)\cos(\tau\delta y_m) - \cos(\tau\delta y_{m+1}) + 2\}, \\ \widetilde{B}_x =& 192\epsilon\lambda_{l,m}\delta x_l\delta_m(1 + \beta\delta y_m)(2 + \beta\delta y_m) \\ & \{(1 + \beta\delta y_m)\sin(\tau\delta y_m) - \sin(\tau\delta y_{m+1})\}, \\ \widetilde{C}_x =& 2\delta y_m^2(2 + \beta\delta y_m)(27\beta^4\delta y_m^4 + 32\beta\delta y_m - 16)(1 + \beta\delta y_m)^3\cos(\tau\delta y_m) \\ & -2\delta y_m^2(1 + \beta\delta y_m)(2 + \beta\delta y_m)(27\beta^4\delta y_m^4 + 48\beta\delta y_m + 16)\cos(\tau\delta y_{m+1}) \\ & -2\delta y_m^2(1 + \beta\delta y_m)(2 + \beta\delta y_m)^2(27\beta^5\delta y_m^5 + 32\beta^2\delta y_m^2 + 80\beta\delta y_m + 80), \\ \widetilde{D}_x =& 2\delta x_l^2(2 + \alpha\delta x_l)(1 + \alpha\delta x_l)^3(27\alpha^4\delta x_l^4 + 32\alpha\delta x_l - 16)\sin(\eta\delta x_l) \\ & +2\delta x_l^2(1 + \alpha\delta x_l)(2 + \alpha\delta x_l)(27\alpha\delta x_l)(27\alpha^4\delta x_l^4 + 48\alpha\delta x_l + 16)\sin(\eta\delta x_{l+1}).\end{aligned}$$

Upon simplification, we get

$$\begin{aligned}\widetilde{A}_x\widetilde{B}_x + \widetilde{C}_x\widetilde{D}_x =& -768\epsilon\lambda_{l,m}\delta x_l^3\delta y_m s_1(1 + \alpha\delta x_l)^3(2 + \alpha\delta x_l)^3\sin^2(\eta\delta x_l/2) \\ & -768\epsilon\lambda_{l,m}\delta x_l^3\delta y_m s_2(1 + \alpha\delta x_l)^2(2 + \alpha\delta x_l)^3\sin^2(\eta\delta x_{l+1}/2) \\ & +768\epsilon\lambda_{l,m}\delta x_l^3\delta y_m s_3(3\alpha\delta x_l + 2)(2 + \alpha\delta x_l)^2. \\ & (1 + \alpha\delta x_l)^3\sin^2\{\eta(\delta x_l + \delta x_{l+1})/2\},\end{aligned} \tag{7.23}$$

where

$$s_1 = 64 + 96\alpha\delta x_l + 64\alpha^2\delta x_l^2 + 27\alpha^4\delta x_l^4 + 54\alpha^5\delta x_l^5,$$
$$s_2 = 64 + 32\alpha\delta x_l + 32\alpha^2\delta x_l^2 - 27\alpha^4\delta x_l^4 + 27\alpha^5\delta x_l^5,$$
$$s_3 = -16 + 8\delta x_l + 4\alpha^2\delta x_l^2 - 6\alpha^3\delta x_l^3 + 9\alpha^4\delta x_l^4.$$

Since $0 < \alpha, \beta < 1$, $\epsilon > 0$, and mesh step-sizes $\delta x_l, \delta y_m \in (0,1)$, we see that $s_1 > 0, s_2 > 0$ and $s_3 < 0$. Therefore, we find $\widetilde{A}_x\widetilde{B}_x + \widetilde{C}_x\widetilde{D}_x < 0$. As a result, we get $|\xi_x| < 1$. Similarly, one can prove $|\xi_y| < 1$. Hence, $|\xi| \leq 1$, and this establishes the unconditional stability of the fourth-order quasi-variable meshes two-level implicit compact scheme applied to transformed (2+1)-dimensions coupled Burger's equation.

8. Numerical simulations and interpretations

This section presents the computed accuracy in the solution values and numerical order obtained for various mesh-step sizes. To solve linear convection-diffusion equations, we have employed alternating direction implicit scheme. The nonlinear Burger's and Boussinesq equations are addressed by the Newton-Raphson method with an initial guess as zero vector. The boundary and initial data are achieved from the theoretical solution, and repetitions halt once the absolute tolerance error 10^{-12} has been achieved [42]. To ease the numerical computations, we will select an equal number of meshes ($L = M$), along the xy-directions. The number of temporal meshes is determined from the relation $J = LM/\lambda_{l,m}, \delta t \approx \lambda_{l,m}\delta x_l \delta y_m$. Therefore, it is viable to measure the accuracy of order four with quasi-variable mesh points by making twice the number of meshes in the subsequent computations. In the numerical simulations, we shall choose the mesh ratio parameter $\lambda_{l,m} = \delta t/\delta x_l \delta y_m = 1.6$, for all l, m. The $\mathcal{L}_\infty$-norm and $\mathcal{L}_2$-norm of errors and order of convergence is obtained by using

$$\mathcal{L}\infty^{(L,M)} = \max_{\substack{1\leq l\leq L\\ 1\leq m\leq M}} \left|W_{l,m}^j - W(x_l, y_m, t_j)\right|, \qquad \Theta_\infty = \log_2\left[\frac{\mathcal{L}_\infty^{(L,M)}}{\mathcal{L}_\infty^{(2L,2M)}}\right]$$

and

$$\mathcal{L}_2^{(L,M)} = \left[\frac{1}{LM}\sum\nolimits_{l=1}^{L}\sum\nolimits_{m=1}^{M}\sum\nolimits_{j=1}^{J}\left(W_{l,m}^j - w_{l,m}^j\right)^2\right]^{1/2}, \Theta_2 = \log_2\left[\frac{\mathcal{L}_2^{L,M}}{\mathcal{L}_2^{(2L,2M)}}\right].$$

In order to generate the difference equations, Maple's *CodeGeneration* package is used while numerical computations are performed in C on the Mac operating system.

Example 8.1 [24,37] We consider the homogeneous convection-diffusion equation

$$\epsilon\left(\frac{\partial^2 W}{\partial x^2} + \frac{\partial^2 W}{\partial y^2}\right) = \frac{\partial W}{\partial t} + a\frac{\partial W}{\partial x} + b\frac{\partial W}{\partial y}, \tag{8.1}$$

possessing the analytic solution

$$W(x,y,t) = \frac{1}{4t+1}\exp\left[-\frac{\left(x - at - \frac{1}{2}\right)^2 + \left(y - bt - \frac{1}{2}\right)^2}{\epsilon(4t+1)}\right]. \tag{8.2}$$

Here, the physical parameters $a = b = 10^{-2}$ and $\epsilon = 10^{-3}, 10^{-4}, 10^{-5}$ are considered for computational purpose, and it refers to the Péclet number, $P_e = a/\epsilon = 10, 10^2, 10^3$. The high Péclet number number brings up negligible diffusion, and uniform meshes high-order scheme yields deteriorating order and accuracies to the solution values. The effect of Péclet number ($10^{-1} \leq P_e \leq 10^2$), on the solution, can be viewed graphically in Figure 1. Experiments with quasi-variable meshes fourth-order implicit compact scheme capture the multiple characters of the solution due to peculiar behavior of mesh location. The results of various values of diffusion coefficients are presented in Table 1 at the time level $t = 1$.

Example 8.2 *Burger's Equation*: It is a nonlinear advection-diffusion equation and appears in the study of dispersion and pollutant transport, wave process in the thermoelastic medium, the formation of structure in the cosmology adhesion model and shock wave. The unsteady two-space dimensions Burgers equation incorporating the interaction between nonlinear convection phenomenon and diffusive viscus processes takes the following form

$$\epsilon\left(\frac{\partial^2 W}{\partial x^2} + \frac{\partial^2 W}{\partial y^2}\right) = \frac{\partial W}{\partial t} + W\left(\frac{\partial W}{\partial x} + \frac{\partial W}{\partial y}\right), 0 \leq x, y \leq 1, t > 0, \tag{8.3}$$

where $\epsilon = R_e^{-1}, 0 < \epsilon \ll 1$, and R_e is the Reynolds number, used to forecast the transition from laminar to turbulent flow. Laminar flow takes place at a low value of Reynolds number, while turbulence is observed with high Reynolds number. For the large Reynolds number, the Burgers equation behaves like a hyperbolic PDE, and solution values depict multiple characters due to the formation of sharp shock-like wavefronts. We compute the solution error using the analytical solution

$$W(x, y, y) = \frac{2\epsilon\pi \sin(\pi(x+y))e^{-2\epsilon\pi^2 t}}{2 + \cos(\pi(x+y)e^{-2\epsilon\pi^2 t}}, \tag{8.4}$$

for small and large value of Reynolds number [34]. The accuracy and numerical order are presented in Table 2 for the different mesh points at the time level $t = 1$. The solution behavior is smooth for small ϵ and $\alpha = \beta = 0$, but for large ϵ, uniform mesh fourth-order scheme results in an oscillatory solution. Thus, quasi-variable mesh fourth-order scheme gained its importance, which produces a stable and convergent solution. The maximum absolute error, at the time level $t = 1$, is reported in Table 2.

Example 8.3 [10, 30] Consider the generalized Burgers-Huxley equation

$$\epsilon\left(\frac{\partial^2 W}{\partial x^2} + \frac{\partial^2 W}{\partial y^2}\right) = \frac{\partial W}{\partial t} + aW^n\left(\frac{\partial W}{\partial x} + \frac{\partial W}{\partial y}\right) + W(W^n - 1)(W^n - \gamma), \tag{8.5}$$

where $a \in \mathbb{R}^+$. denotes the coefficient of advection, $\gamma \in (0, 1)$ and $n \geq 1$, are parameters. For $\epsilon = 1$, it possess an analytic solution

$$W(x, y, t) = \left[\frac{\gamma}{2} + \frac{\gamma}{2}\tanh\left\{\sigma\gamma\left((x+y)/\sqrt{2} - ct\right)\right\}\right]^{1/n}, \tag{8.6}$$

where

$$\rho = \sqrt{2a^2 + 4n + 4},\ \sigma = \frac{n\left(\rho - \sqrt{2}a\right)}{(4n+4)} \text{ and } c = \frac{\left[\gamma(\sqrt{2}a - \rho) + (\sqrt{2}a + \rho)(n+1)\right]}{(2n+2)}.$$

The accuracies in analytic and approximate solution values are determined for $n = 2$ and $\gamma = 0.5$. Experiments with small advection coefficient a result in stable behavior of solutions, while the larger values of a exhibit instability while implementing uniform meshes fourth-order compact scheme (4.9) with $\alpha = \beta = 0$. In Table 3, we have presented $\mathcal{L}_\infty$- and $\mathcal{L}_2$- norm of errors with convergence order for $a = 10^4$ and various number of mesh points.

Example 8.4 *Burgers-Fisher equation* (BFE): In the ecology, BFE combines the logistic growth and diffusion to model the proliferation and population spread [49,50]. BFE has a convective property from Burgers equation, reaction and diffusion transport from the Fisher equation. The mathematical equation is given by

$$\epsilon\left(\frac{\partial^2 W}{\partial x^2}+\frac{\partial^2 W}{\partial y^2}\right)=\frac{\partial W}{\partial t}+aW^n\left(\frac{\partial W}{\partial x}+\frac{\partial W}{\partial y}\right)+bW(W^n-1), \tag{8.7}$$

and

$$W(x,y,t)=\left[\frac{1}{2}+\frac{1}{2}\tanh\left\{r(x-y-qt)\right\}\right]^{1/n},$$
$$r=-\frac{an}{2\epsilon(1+n)},\quad q=\frac{b\epsilon(1+n)^2+2a^2}{a(1+n)},$$

is the analytic solution. In Table 4, we have performed simulations for various combinations of the parameters (ϵ, a, b, n). For $(\epsilon, a, b, n) = (1, 1, 1, 2)$, the solution behavior is smooth with uniform mesh, and there is no need to refine the meshes in the high-order implicit compact scheme. However, as the values of a, b, n increase or ϵ decreases, the numerical solution's instability arises, and it necessitates the mesh refinement by choosing a non-zero mesh stretching ratio.

Example 8.5 (Polyanin and Zaitsev [39]) Boussinesq equation: The model described the unsteady flow inside free surface porous media and appears in nonlinear heat conduction theory

$$\frac{\partial}{\partial x}\left(W\frac{\partial W}{\partial x}\right)+\frac{\partial}{\partial y}\left(W\frac{\partial W}{\partial y}\right)=\frac{\partial W}{\partial t},\quad 0<x,y<1,\quad t>0. \tag{8.8}$$

The initial and boundary values are taken from the analytic solution $W(x, y, t) = (2x + y + t + 1)/5$. Simulations with uniform meshes fourth-order scheme ($\alpha = \beta = 0$) result in an oscillatory solution. In contrast, the quasi-variable meshes fourth-order compact scheme yields order-preserving solution values. At the time level $t = 1$, numerical order and absolute errors are shown in Table 5.

Example 8.6 (Fisher and Bialecki [13]) *Coupled Burgers Equation*: We shall compute the numerical solution values of equation (7.1)-(7.2) and measure the absolute errors and numerical convergence order using the analytic solutions

$$U(x,y,t)=\frac{3}{4}-\frac{1}{4}\left[1+e^{\{-4(x-y)-t\}/\{32\epsilon\}}\right]^{-1},$$
$$V(x,y,t)=\frac{3}{4}+\frac{1}{4}\left[1+e^{\{-4(x-y)-t\}/\{32\epsilon\}}\right]^{-1}. \tag{8.9}$$

Computational tests are performed over the domain $\Omega\times(0,T)$, with $T = 1$, for many mesh arrangements. It is noted that the order and solution accuracies confirm with

the low value of the Reynolds number $R_e = 1/\epsilon$, say $R_e = 10$. However, with a large value of Reynolds number $Re = 10^2$ and 10^3, the equi-spaced distribution of mesh points in the fourth-order compact scheme yields high oscillations in the solution. To achieve the expected accuracy, we need to implement an amply small size of mesh stencils and massive computing time in turn. A minor modification in the mesh-point locations makes it feasible to achieve more accurate solution values with the desired accuracy by increasing Reynolds number's value, keeping very few mesh points. Table 6 presents an average of $\mathcal{L}_\infty$-norm and $\mathcal{L}_2$-norm errors in $U(x, y, t)$ and $V(x, y, t)$, and corresponding convergence order for different values of ϵ. It may be concluded that approximated solution values obtained by the quasi-variable meshes high-order implicit compact scheme are concurrent with analytic solution values up to the fourth-order accuracy.

9. Conclusion

We have described an optimum convergence order splitting compact operator scheme that implements a variable mesh spacing for solving mildly nonlinear two-dimensions parabolic PDEs in the present work. Our difficulty encountered in the operator splitting scheme on variable mesh spacing. By considering the variable mesh spacing, such as $\delta x_{l+1} = \alpha x_l, \delta y_{m+1} = \beta y_m$, (exponential expanding meshes) discussed by Fukuyo [15, 16], it is possible to achieve a third-order compact formulation. Still, operator splitting formulation in this category of meshes is not possible, leading to an inefficient system of difference equations. The new variable mesh spacing, high-order truncation error, and compact formulation make the proposed scheme more efficient, especially when the problems possess layer behavior. The present scheme can achieve a more accurate solution with reduced computing time than a standard fourth-order compact scheme obtained on uniform fine mesh points. An a priori error estimate is obtained that shows the fourth-order convergence of solution values as $\|\delta x\|, \|\delta y\|, \delta t \to 0$ and $\delta t \propto \delta x_l \delta y_m \; \forall l, m$. The computational experiments, intended to investigate the beauty of the implicit compact scheme, concord the theoretical analysis, and the new procedure offers an efficient solution given memory and data space.

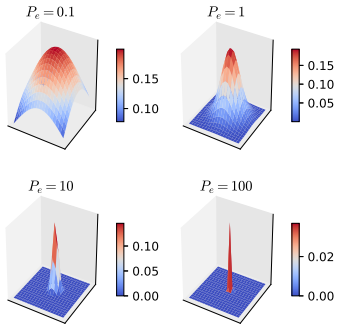

Figure 1. Approximate solution surface with changing value of ϵ

Table 1. Error estimates and numerical order in Example 8.1

L	α	β	$\|\|\mathcal{L}\|\|_\infty^{(L,M)}$	$\|\|\mathcal{L}\|\|_2^{(L,M)}$	Θ_∞	Θ_2
$a = b = 10^{-2}, \epsilon = 10^{-3}$						
4	0.0000	0.0000	$6.99e-01$	$2.35e-01$	$--$	$--$
8	0.0000	0.0000	$5.06e-01$	$7.54e-02$	0.5	1.6
16	0.0000	0.0000	$1.34e-01$	$9.98e-03$	1.9	2.9
32	0.0000	0.0000	$2.21e-03$	$1.17e-04$	5.9	6.4
4	0.2600	0.4000	$1.59e-02$	$5.34e-03$	$--$	$--$
8	0.2300	0.1900	$8.66e-04$	$1.24e-04$	4.2	5.4
16	0.0880	0.0880	$4.84e-05$	$3.23e-06$	4.2	5.3
32	0.0300	0.0382	$2.53e-06$	$1.25e-07$	4.3	4.7
$a = b = 10^{-2}, \epsilon = 10^{-4}$						
4	0.0000	0.0000	$7.86e-01$	$2.72e-01$	$--$	$--$
8	0.0000	0.0000	$6.58e-01$	$1.00e-01$	0.26	1.4
16	0.0000	0.0000	$5.36e-01$	$4.05e-02$	0.29	1.3
32	0.0000	0.0000	$3.02e-01$	$1.24e-02$	0.83	1.7
4	0.3810	0.4000	$1.39e-02$	$4.65e-03$	$--$	$--$
8	0.1200	0.0900	$7.67e-04$	$1.33e-04$	4.2	5.1
16	0.0200	0.0820	$1.11e-05$	$2.24e-06$	4.2	5.6
32	0.0180	0.0375	$1.85e-06$	$1.07e-07$	4.5	4.7
$a = b = 10^{-2}, \epsilon = 10^{-5}$						
4	0.0000	0.0000	$9.80e-01$	$4.53e-01$	$--$	$--$
8	0.0000	0.0000	$8.52e-01$	$1.54e-01$	0.20	1.6
16	0.0000	0.0000	$5.38e-01$	$5.33e-02$	0.66	1.5
32	0.0000	0.0000	$3.25e-01$	$2.20e-02$	0.72	1.3
4	0.0000	0.0000	$9.80e-01$	$4.53e-01$	$--$	$--$
8	0.0300	0.0040	$9.34e-02$	$1.60e-02$	3.4	4.8
16	0.0190	0.0390	$7.93e-03$	$5.29e-04$	3.6	4.9
32	0.0000	0.0020	$5.41e-04$	$2.75e-05$	3.9	4.3

Table 2. Error estimates and numerical order in Example 8.2

L	α	β	$\|\|\mathcal{L}\|\|_\infty^{(L,M)}$	$\|\|\mathcal{L}\|\|_2^{(L,M)}$	Θ_∞	Θ_2
	$\epsilon = 10^{-3}$					
4	0.000	0.000	$1.06e-06$	$5.10e-07$	$--$	$--$
8	0.000	0.000	$2.82e-07$	$1.53e-07$	1.9	1.7
16	0.000	0.000	$2.92e-08$	$1.47e-08$	3.3	3.4
32	0.000	0.000	$2.08e-09$	$7.77e-10$	3.8	3.9
	$\epsilon = 10^{-2}$					
4	0.000	0.000	$5.35e-05$	$2.53e-05$	$--$	$--$
8	0.000	0.000	$8.12e-06$	$4.67e-06$	2.7	2.4
16	0.000	0.000	$7.12e-07$	$3.64e-07$	3.5	3.7
32	0.000	0.000	$4.73e-08$	$2.32e-08$	3.9	4.0
	$\epsilon = 10^{-1}$					
4	0.000	0.000	$1.95e-04$	$1.59e-04$	$--$	$--$
8	0.000	0.000	$1.57e-05$	$9.34e-06$	3.6	4.1
16	0.000	0.000	$1.05e-06$	$5.56e-07$	3.9	4.1
32	0.000	0.000	$6.66e-08$	$3.38e-08$	4.0	4.0
	$\epsilon = 10$					
4	0.380	0.380	$2.91e-03$	$2.17e-03$	$--$	$--$
8	0.170	0.130	$1.70e-04$	$4.12e-05$	4.1	5.7
16	0.070	0.079	$9.11e-06$	$3.61e-06$	4.2	3.5
32	0.033	0.035	$5.00e-07$	$2.46e-07$	4.2	3.9
	$\epsilon = 10^2$					
4	0.530	0.530	$2.32e-00$	$1.87e-00$	$--$	$--$
8	0.400	0.410	$1.30e-01$	$5.20e-02$	4.2	5.2
16	0.066	0.060	$6.68e-03$	$9.51e-04$	4.3	5.8
32	0.034	0.034	$3.64e-04$	$3.59e-05$	4.2	4.7

Table 3. Error estimates and numerical order in Example 8.3, $\beta = 2, \gamma = 0.5$

L	α	β	$\|\|\mathcal{L}\|\|_{\infty}^{(L,M)}$	$\|\|\mathcal{L}\|\|_{2}^{(L,M)}$	Θ_{∞}	Θ_2
	$\alpha = 10^1$					
4	0.0000	0.0000	$7.44e-07$	$5.58e-07$	$--$	$--$
8	0.0000	0.0000	$4.65e-08$	$3.02e-08$	4.0	4.2
16	0.0000	0.0000	$2.95e-09$	$1.76e-09$	4.0	4.1
32	0.0000	0.0000	$1.84e-10$	$1.06e-10$	4.0	4.0
	$\alpha = 10^2$					
4	0.000	0.0000	$3.71e-07$	$2.44e-07$	$--$	$--$
8	0.0000	0.0000	$2.63e-08$	$1.52e-08$	3.8	4.0
16	0.0000	0.0000	$2.66e-09$	$8.04e-10$	4.0	4.1
32	0.0000	0.0000	$1.05e-10$	$5.47e-11$	4.0	4.0
	$\alpha = 10^3$					
4	0.000	0.1400	$9.90e-07$	$5.57e-07$	$--$	$--$
8	0.000	0.0020	$8.58e-08$	$5.57e-08$	3.5	3.3
16	0.000	0.0001	$6.10e-09$	$3.08e-09$	3.8	4.2
32	0.000	$5.5e-06$	$3.27e-10$	$1.50e-10$	4.2	4.4
	$\alpha = 10^4$					
4	0.8000	0.8000	$2.71e-07$	$1.33e-07$	$--$	$--$
8	0.0100	0.0010	$1.65e-08$	$7.67e-09$	4.0	4.1
16	0.0000	$1.00e-04$	$1.23e-09$	$5.69e-10$	3.7	3.8
32	0.0000	$5.50e-06$	$8.58e-11$	$4.14e-11$	3.8	3.8

Table 4. Error estimates and numerical order in Example 8.5

L	α	β	$\|\|\mathcal{L}\|\|_\infty^{(L,M)}$	$\|\|\mathcal{L}\|\|_2^{(L,M)}$	Θ_∞	Θ_2
$\epsilon = a = b = 1, n = 2$						
4	0.0000	0.0000	$4.65e-05$	$3.48e-05$	$--$	$--$
8	0.0000	0.0000	$2.90e-06$	$1.88e-06$	4.0	4.2
16	0.0000	0.0000	$1.85e-07$	$1.09e-07$	4.0	4.1
32	0.0000	0.0000	$9.51e-09$	$5.53e-09$	4.3	4.3
$\epsilon = 1, a = b = 10, n = 2$						
4	0.9700	0.9700	$1.23e-02$	$8.96e-03$	$--$	$--$
8	0.9600	0.2200	$7.18e-04$	$1.80e-04$	4.1	5.6
16	0.0200	0.0870	$4.21e-05$	$6.62e-06$	4.1	4.8
32	0.0200	0.0428	$1.64e-06$	$3.82e-07$	4.7	4.1
$\epsilon = 1, a = b = 10, n = 4$						
4	0.8000	0.8000	$3.08e-03$	$1.71e-03$	$--$	$--$
8	0.2000	0.5000	$1.35e-04$	$4.02e-05$	4.5	5.4
16	0.0200	0.0830	$6.32e-06$	$1.39e-06$	4.4	4.9
32	0.0200	0.0372	$3.46e-07$	$6.33e-08$	4.2	4.5
$\epsilon = 0.04, a = b = 1, n = 2$						
4	0.0000	0.0000	$6.47e-02$	$3.52e-02$	$--$	$--$
8	0.0000	0.0000	$2.56e-02$	$5.29e-03$	1.3	1.9
16	0.0000	0.0000	$2.72e-03$	$7.30e-04$	3.2	3.7
32	0.0000	0.0000	$1.83e-04$	$4.66e-05$	3.9	4.0
$\epsilon = 0.06, a = b = 1, n = 2$						
4	0.0000	0.0000	$2.71e-02$	$1.61e-02$	$--$	$--$
8	0.0000	0.0000	$5.23e-03$	$1.90e-03$	2.4	3.1
16	0.0000	0.0000	$4.02e-04$	$1.28e-04$	3.7	3.9
32	0.0000	0.0000	$2.59e-05$	$7.96e-06$	4.0	4.0

Table 5. Error estimates and numerical order in Example 8.5

L	α	β	$\|\|\mathcal{L}\|\|_\infty^{(L,M)}$	$\|\|\mathcal{L}\|\|_2^{(L,M)}$	Θ_∞	Θ_2
4	0.0000	$6.01e-01$	$1.57e-02$	$1.06e-02$	$--$	$--$
8	0.0000	$9.00e-03$	$9.09e-04$	$5.87e-04$	4.1	4.2
16	0.0000	$3.00e-04$	$7.09e-05$	$4.22e-05$	3.7	3.8
32	0.0000	$1.00e-07$	$5.59e-06$	$2.84e-06$	3.7	3.9

Table 6. Error estimates and numerical order in Example 8.5

L	α	β	$\|\|\mathcal{L}\|\|_\infty^{(L,M)}$	$\|\|\mathcal{L}\|\|_2^{(L,M)}$	Θ_∞	Θ_2
	$\epsilon = 10^{-1}$					
4	0.0000	0.0000	$7.72e-06$	$8.85e-06$	$--$	$--$
8	0.0000	0.0000	$7.74e-07$	$1.12e-06$	3.3	3.0
16	0.0000	0.0000	$6.15e-08$	$1.18e-07$	3.7	3.2
32	0.0000	0.0000	$4.26e-09$	$1.12e-08$	3.9	3.4
	$\epsilon = 10^{-2}$					
4	0.9300	0.2500	$7.11e-01$	$5.12e-01$	$--$	$--$
8	0.2000	0.2500	$4.51e-02$	$4.60e-02$	4.0	3.5
16	$8.0e-03$	0.0010	$3.19e-03$	$4.68e-03$	3.8	3.3
32	$1.9e-04$	$6.0e-05$	$3.09e-04$	$5.53e-04$	3.4	3.1
	$\epsilon = 10^{-3}$					
4	0.7000	0.900	$9.44e-02$	$7.79e-02$	$--$	$--$
8	0.3300	0.2900	$9.43e-03$	$8.33e-03$	3.3	3.2
16	0.0962	0.0893	$9.44e-04$	$5.33e-04$	3.3	4.0

Appendix A: Values of coefficients $\sigma_{l+p,m+s} \in \mathcal{J}$ in equation (3.16)

$\sigma_{l,m}$	$[\zeta + 3(1+\beta\delta y_m)(1+\alpha\delta x_l+\alpha^2\delta x_l^2) + 3(1+\alpha\delta x_l)$ $(1+\beta\delta y_m+\beta^2\delta y_m^2)]/[9(1+\alpha\delta x_l)], \zeta = \alpha^2\beta^2\delta x_l^2\delta y_m^2$
$\sigma_{l+1,m}$	$2\alpha\beta^2\delta x_l\delta y_m^2 + 3(1+3\alpha\delta x_l)(1+\beta\delta y_m)/[18(1+\alpha\delta x_l)$ $(2+\alpha\delta x_l)(1+\beta\delta y_m)]$,
$\sigma_{l,m+1}$	$2\alpha^2\beta^2\delta x_l^2\delta y_m + 3(1+3\alpha\delta x_l)(1+\beta\delta y_m)/[18(1+\alpha\delta x_l)$ $(1+\beta\delta y_m)(2+\beta\delta y_m)]$,
$\sigma_{l-1,m}$	$(1+\alpha\delta x_l)[3(1-2\alpha\delta x_l)(1+\beta\delta y_m) - 2\alpha\beta^2\delta x_l\delta y_m^2]/$ $[18(2+\alpha\delta x_l)(1+\beta\delta y_m)]$,
$\sigma_{l,m-1}$	$(1+\beta\delta y_m)[3(1+\alpha\delta x_l)(1-2\beta\delta y_m) - 2\alpha^2\beta\delta x_l^2\delta y_m/$ $[18(1+\alpha\delta x_l)(2+\beta\delta y_m)]$,
$\sigma_{l+1,m+1}$	$\alpha\beta\delta x_l\delta y_m/[9(2+\alpha\delta x_l)(2+\beta\delta y_m)(1+\alpha\delta x_l)(1+\beta\delta y_m)]$,
$\sigma_{l+1,m-1}$	$-\alpha\beta\delta x_l\delta y_m(1+\beta\delta y_m)/[9(2+\alpha\delta x_l)(2+\beta\delta y_m)(1+\alpha\delta x_l)]$,
$\sigma_{l-1,m+1}$	$-\alpha\beta\delta x_l\delta y_m(1+\alpha\delta x_l)/[9(2+\alpha\delta x_l)(2+\beta\delta y_m)(1+\beta\delta y_m)]$,
$\sigma_{l-1,m-1}$	$\alpha\beta\delta x_l\delta y_m(1+\alpha\delta x_l)(1+\beta\delta y_m)/[9(2+\alpha\delta x_l)(2+\beta\delta y_m)]$,

Appendix B: Values of $S_i^0, S_i^{\pm}, Z_i, Z_k^0$ appearing in equation (5.10)-(5.11)

$$S_1^{\pm} = \begin{bmatrix} B \pm B_y\delta y_m - B_x\delta x_l & C \pm C_y\delta y_m - (B + C_x)\delta x_l & D - D_x\delta x_l \pm (D_y + B)\delta y_m \\ B \pm B_y\delta y_m & C \pm C_y\delta y_m & D \pm (D_y + B)\delta y_m \\ B \pm B_y\delta y_m + B_x\delta x_l & C \pm C_y\delta y_m + (B + C_x)\delta x_l & D + D_x\delta x_l \pm (D_y + B)\delta y_m \end{bmatrix}$$

$$S_2^{\pm} = \begin{bmatrix} E \pm E_y\delta y_m - E_x\delta x_l & -E\delta x_l & \pm 2D \\ E \pm E_y\delta y_m & 0 & \pm 2D \\ E \pm E_y\delta y + E_x\delta x_l & E\delta x_l & \pm 2D \end{bmatrix}, Z_1^0 = \rho\delta t \begin{bmatrix} W_{l,m}^{t^j} \\ W_{l,m}^{xt^j} \\ W_{l,m}^{yt^j} \end{bmatrix}, \delta^* = 3\beta\delta y_m + 2$$

$$S_3^{\pm} = \begin{bmatrix} (\alpha\delta x_l + 2)C - 2(C_x\delta x_l - C_y\delta y_m) & \delta^* D + 2(D_y\delta y_m \pm D_x\delta x_l) & -2D\delta x_l \\ -(\alpha\delta x_l + 1)C - C_y\delta y_m & \delta^* D \pm 2D_y\delta y_m & 0 \\ (3\alpha\delta x_l + 2)C + 2(C_x\delta x_l + C_y\delta y_m) & \delta^* D \pm 2(D_y\delta y_m + D_x\delta x_l) & 2D\delta x_l \end{bmatrix}$$

$$S_4^{\pm} = \begin{bmatrix} -C_x\delta x_l & -(D\delta x_l \mp C\delta y_m) & C/12 \\ 0 & \pm C\delta y_m & 0 \\ C\delta x_l & D\delta x_l \pm C\delta y_m & -C/12 \end{bmatrix}, \quad S_5^{\pm} = \begin{bmatrix} A - A_x\delta x_l \pm A_y\delta y_m \\ A \pm A_y\delta y_m \\ A + A_x\delta x_l \pm A_y\delta y_m \end{bmatrix}$$

$$S_1^0 = \begin{bmatrix} B - B_x\delta x_l & C - (C_x + B)\delta x_l & D - D_x\delta x_l \\ B & C & D \\ B + B_x\delta x_l & C + (C_x + B)\delta x_l & D + D_x\delta x_l \end{bmatrix}, \quad S_2^0 = \begin{bmatrix} E - \delta x_l E_x & -E\delta x_l & 2A \\ E & 0 & 2A \\ E + \delta x_l E_x & E\delta x_l & 2A \end{bmatrix}$$

$$S_3^0 = \begin{bmatrix} (\alpha\delta x_l + 2)C - 2C_x\delta x_l & -(\beta\delta y_m + 1)D + D_x\delta x_l & D\delta x_l \\ -(\alpha\delta x_l + 1)C & -(\beta\delta y_m)D & 0 \\ (3\alpha\delta x_l + 2)C + 2C_x\delta x_l & -(\beta\delta y_m + 1)D - D_x\delta x_l & -D\delta x_l \end{bmatrix}$$

$$S_4^0 = \begin{bmatrix} -12 & -12 & 1 \\ 0 & 0 & 0 \\ 12 & 12 & -1 \end{bmatrix}, S_5^0 = \begin{bmatrix} -1 \\ 0 \\ 1 \end{bmatrix}, S_6^{\pm} = \begin{bmatrix} -4 & -1 & 6 \\ -2 & -1 & 6 \\ -4 & -1 & 6 \end{bmatrix}, \begin{bmatrix} Z_1 \\ Z_5 \end{bmatrix} = \begin{bmatrix} Z_1^0 \\ \rho\delta t \\ A_x\rho\delta x_l\delta t \\ Z_5^0 \end{bmatrix}$$

$$Z_2^0 = \frac{\delta t}{2}\begin{bmatrix} W_{l,m}^{tt^j} \\ W_{l,m}^{xtt^j} \\ \rho \end{bmatrix}, Z_3^0 = -\frac{1}{6}\begin{bmatrix} \delta x_l^2 W_{l,m}^{xxx^j} \\ \delta y_m^2 W_{l,m}^{yyy^j} \\ \delta y_m^2 W_{l,m}^{xyyy^j} \end{bmatrix}, Z_4^0 = -\frac{\delta x_l}{12}\begin{bmatrix} C\rho\delta t W_{l,m}^{xx^j} \\ D\rho\delta t W_{l,m}^{xyt^j} \\ C\delta x_l^2 W_{l,m}^{xxxx^j} \end{bmatrix}$$

$$Z_2 = \delta t\begin{bmatrix} W_{l,m}^{tt^j} \\ W_{l,m}^{xtt^j} \\ \rho\delta y_m W_{l,m}^{yy^j} \end{bmatrix}, Z_3 = \mathbf{Z_3^0}, Z_4 = \begin{bmatrix} \rho\delta t W_{l,m}^{xxt^j} \\ \rho\delta t W_{l,m}^{xyt^j} \\ \delta x_l^3 W_{l,m}^{xxxx^j} \end{bmatrix}, Z_6 = \delta y_m \begin{bmatrix} C\delta x_l^2 W_{l,m}^{xxxy^j} \\ D\delta y_m^2 W_{l,m}^{yyyy^j} \\ E\delta t W_{l,m}^{ytt^j} \end{bmatrix}$$

Appendix C: Expression of $P_i, Q_i, R_{p,s}, i = 1(1)8, (p,s) \in \mathcal{J}$ in (6.9)-(6.10)

P_1	$\alpha\delta t/2\delta x_l + \alpha\delta x_l(27\alpha^3\delta x_l^3 + 32)/96 - \alpha\delta x_l(\alpha^2\delta x_l^2 - \beta^3\delta y_m^3)/24\epsilon$ $- \alpha\delta x_{l+1}(\beta^2\delta y_m^2 + 2)/24\epsilon$
P_2	$1/12 - \epsilon\delta t/2\delta x_l^2 + \alpha(2a\delta t + \delta x_l)/12 - a(\alpha\delta x_l + 1)(\alpha\delta x_l^2 + a\delta t)/24\epsilon$
P_3	$b\delta t/2\delta y_m + \beta\delta y_m(27\beta^3\delta y_m^3 + 32)/96 + \beta\delta y_m(\alpha^3\delta x_l^3 - \beta^2\delta y_m^2)/24\epsilon$ $- b\delta y_{m+1}(\delta x_l^2\alpha^2 + 2)/24\epsilon$
P_4	$1/12 - \epsilon\delta t/2\delta y_m^2 + \beta(2b\delta t + \delta y_m)/12 - b(\beta\delta y_{m+1})(\beta\delta y_m^2 + b\delta t)/24\epsilon$
P_5	$a\delta t\delta x_{l+1}/24\delta y_m^2 + a\delta t(\beta\delta y_m + 1)/24\delta x_l - \epsilon\alpha\delta t\delta x_l/6\delta y_m^2$
P_6	$b\delta t y_{m+1}/24\delta x_l^2 + b\delta t(\alpha\delta x_l + 1)/24\delta y_m - \epsilon\beta\delta t\delta y_m/6\delta x_l^2$
P_7	$\alpha\beta\delta x_l\delta y_m/9 + \delta t(\alpha\beta\delta y_m^2 + b\alpha\delta x_l^2)/6\delta x_l\delta y_m - ab\delta t(\delta x_l\delta x_{l+1}$ $+\delta y_m\delta y_{m+1})/24\epsilon\delta x_l\delta y_m$
P_8	$-\epsilon\delta t(\alpha\delta x_l + 1)/24\delta x_l^2 - \epsilon\delta t(1 + \beta\delta y_m)/24\delta x_l^2$
Q_1	$-a\delta t/2\delta x_l + \alpha\delta x_l(27\alpha^3\delta x_l^3 + 32)/96 - a\delta x_l(\alpha^2\delta x_l^2 - \beta^3\delta y_m^3)/24\epsilon$ $- a\delta x_{l+1}(\beta^2\delta y_m^2 + 2)/24\epsilon$
Q_2	$1/12 + \epsilon\delta t/2\delta x_l^2 - \alpha(2a\delta t - \delta x_l)/12 - a(1 + \alpha\delta x_l)(\alpha\delta x_l^2 - a\delta t)/24\epsilon$
Q_3	$-b\delta t/2\delta y_m + \beta\delta y_m(27\beta^3\delta y_m^3 + 32)/96 + b\delta y_m(\alpha^3\delta x_l^3 - \beta^2\delta y_m^2)/24\epsilon$ $- b\delta y_{m+1}(\delta x_l^2\alpha^2 + 2)/24\epsilon$
Q_4	$1/12 + \epsilon\delta t/2\delta y_m^2 - \beta(2b\delta t - \delta y_m)/12 + b(\beta\delta y_m + 1)(b\delta t - \beta\delta y_m^2)/24\epsilon$
Q_5	$-P_5$
Q_6	$-P_6$
Q_7	$\alpha\beta\delta x_l\delta y_m/9 - \delta t(\alpha\beta\delta y_m^2 + b\alpha\delta x_l^2)/6\delta x_l\delta y_m + ab\delta t(\delta x_l\delta x_{l+1}$ $+\delta y_m\delta y_{m+1})24\epsilon\delta x_l\delta y_m$
Q_8	$-P_8$
$R^j_{l,m}$	$[\alpha^2\delta x_l^2(\alpha\delta x_l - 1) + \beta^2\delta y_m^2(\beta\delta y_m - 1) - 2]\delta t/3$
$R^j_{l+1,m}$	$[-1/12 + \alpha^2\delta x_l^3(a - 27\alpha\epsilon)/96\epsilon + \alpha\delta x_l^2(a + 11\alpha\epsilon)/48\epsilon + \{\beta^2\delta y_m^2(3a$ $- 8\alpha\epsilon) + 6(a - 3\alpha\epsilon)\}\delta x_l/144\epsilon]\delta t$
$R^j_{l-1,m}$	$[-1/12 + \alpha^2\delta x_l^3(a + 5\alpha\epsilon)/96\epsilon - \alpha\delta x_l^2(a - 5\alpha\epsilon)/48\epsilon - \{\beta^2\delta y_m^2(3a$ $- 8\alpha\epsilon) + 6(a - 3\alpha\epsilon)\}\delta x_l/144\epsilon]\delta t$
$R^j_{l,m+1}$	$[-1/12 + \beta^2\delta y_m^3(b - 27\beta\epsilon)/96\epsilon + \beta\delta y_m^2(b + 11\beta\epsilon)/48\epsilon + \{\alpha^2\delta x_l^2(3b$ $- 8\beta\epsilon + 6(b - 3\beta\epsilon)\delta y_m/144\epsilon]\delta t$
$R^j_{l,m-1}$	$[-1/12 - \beta^2\delta y_m^3(b + 5\beta\epsilon)/96\epsilon - \beta\delta y_m^2(b - 5\beta\epsilon)/48\epsilon - \{\alpha^2\delta x_l^2(3b$ $- 8\beta\epsilon + 6(b - 3\beta\epsilon)\delta y_m/144\epsilon]\delta t$
$R^j_{l+1,m+1}$	$\alpha\beta\delta x_l\delta y_m[3(\alpha\delta x_l + \beta\delta y_m) - 2]\delta t/72$
$R^j_{l-1,m+1}$	$\alpha\beta\delta x_l\delta y_m[\alpha\delta x_l - 3\beta\delta y_m + 2]\delta t/72$
$R^j_{l+1,m-1}$	$\alpha\beta\delta x_l\delta y_m[3\alpha\delta x_l - \beta\delta y_m - 2]\delta t/72$
$R^j_{l-1,m-1}$	$-\alpha\beta\delta x_l\delta y_m[\alpha\delta x_l + \beta\delta y_m + 2]\delta t/72$

References

[1] R. Abazari and M. Abazari, *Numerical study of Burgers–Huxley equations via reduced differential transform method*, Computational and Applied Mathematics, 2013, 32, 1–17.

[2] H. P. Bhatt and A. Q. M. Khaliq, *Fourth-order compact schemes for the numerical simulation of coupled Burgers' equation*, Computer Physics Communications, 2016, 200, 117–138.

[3] L. K. Bieniasz, *A set of compact finite-difference approximations to first and second derivatives related to the extended Numerov method of Chawla on nonuniform grids*, Computing, 2007, 81, 77–89.

[4] N. F. Britton, *Reaction-Diffusion equations and their applications to Biology*, Academic Press, New York, 1986.

[5] D. Britz, *Digital simulation in electrochemistry*, Springer, Berlin, 2005.

[6] C. Clavero and J. C. Jorge, *Another uniform convergence analysis technique of some numerical methods for parabolic singularly perturbed problems*, Computers & Mathematics with Applications, 2015, 70(3), 222–235.

[7] J. D. Cole, *On a quasi-linear parabolic equation occurring in aerodynamics*, Quarterly of Applied Mathematics, 1951, 9(3), 225–236.

[8] M. Dehghan and A. Mohebbi, *High-order compact boundary value method for the solution of unsteady convection–diffusion problems*, Mathematics and Computers in Simulation, 2008, 79(3), 683–699.

[9] Y. Duan and R. Liu, *Lattice Boltzmann model for two-dimensional unsteady Burgers' equation*, Journal of Computational and Applied Mathematics, 2007, 206(1), 432–439.

[10] V. J. Ervin, J. E. M. Díaz and J. Ruiz-Ramírez, *A positive and bounded finite element approximation of the generalized Burgers–Huxley equation*, Journal of Mathematical Analysis and Applications, 2015, 424(2), 1143–1160.

[11] S. E. Esipov, *Coupled Burgers equations: a model of polydispersive sedimentation*, Physical Review E, 1995, 52(4), 3711–3718.

[12] J. H. Ferziger and M. Peric, *Computational methods for fluid dynamics*. Springer-Verlag, Berlin, 2002.

[13] N. Fisher and B. Bialecki, *Extrapolated ADI Crank–Nicolson orthogonal spline collocation for coupled Burgers' equations*, Journal of Difference Equations and Applications, 2020, 26(1), 45–73.

[14] C. A. J. Fletcher, *Generating exact solution of the two-dimensional Burger's equations*, International Journal for Numerical Methods in Fluids, 1983, 3(3), 213–216.

[15] K. Fukuyo, *Stability of Saul'yev's methods with nonuniform grids*, Numerical Heat Transfer, Part B: Fundamentals, 2007, 52(4), 341–352.

[16] K. Fukuyo, *Conditional stability of Larkin methods with non-uniform grid*, Theoretical and Applied Mechanics, 2010, 37(2), 139–159.

[17] J. Geiser, *Higher-order difference and higher-order splitting methods for 2D parabolic problems with mixed derivatives*, International Mathematical Forum, 2007, 67, 3339–3350.

[18] W. Hundsdorfer and J. G. Verwer, *Numerical Solution of Time-Dependent Advection-Diffusion-Reaction Equations*, Springer-Verlag, Berlin, 2003.

[19] N. Jha and L. K. Bieniasz, *A fifth(six) order accurate, three-point compact finite difference scheme for the numerical solution of sixth order boundary value problems on geometric meshes*, Journal of Scientific Computing, 2015, 64, 898–913.

[20] N. Jha and N. Kumar, *An exponential expanding meshes sequence and finite difference method adopted for two-dimensional elliptic equations*, International Journal of Modeling, Simulation, and Scientific Computing, 2016, 7(2), 17 pages.

[21] N. Jha and N. Kumar, *A fourth-order accurate quasi-variable mesh compact finite-difference scheme for two-space dimensional convection-diffusion problems*, Advances in Difference Equations, 2017, 64, 13 pages.

[22] N. Jha and M. Wagley, *Numerical algorithm for coupled viscous Burgers equation using quasi-variable meshes compact operators*, Azerbaijan Journal of Mathematics, 2021, 145–156.

[23] R. Jiwari, S. Pandit and M. E. Koksal, *A class of numerical algorithms based on cubic trigonometric B-spline functions for numerical simulation of nonlinear parabolic problems*, Computational and Applied Mathematics, 2019, 38, 140, 22 pages.

[24] S. Karaa and J. Zhang, *High order ADI method for solving unsteady convection–diffusion problems*, Journal of Computational Physics, 2004, 198(1), 1–9.

[25] H. O. Kreiss and T. A. Manteuffel, *Supra-Convergent Schemes on Irregular Grids*, Mathematics of Computation, 1986, 47, 537–554.

[26] J. D. Lambert, *Numerical methods for ordinary differential systems: the initial value problem*, John Wiley & Sons Ltd., London, 1991.

[27] J. Li, *Geometric Properties and Exact Travelling Wave Solutions for the Generalized Burger-Fisher Equation and the Sharma-Tasso-Olver Equation*, Journal of Nonlinear Modeling and Analysis, 2019, 1(1), 1–10.

[28] B. Liu, R. Wu and L. Chen, *Weak Solutions of a Reaction Diffusion System with Superdiffusion and Its Optimal Control*, Journal of Nonlinear Modeling and Analysis, 2019, 1(2), 271–282.

[29] M. Ma, W. Ma and X Wang, *A compact alternate direct implicit difference method for solving parabolic equation of multi-dimension*, Applied Mathematics and Computation, 2009, 212(2), 281–286.

[30] J. E. Macías-Díaz and A. E. González, *Some remarks on an exact and dynamically consistent scheme for the Burgers-Huxley equation in higher dimensions*, Advances in Difference Equations, 2015, 386, 10 pages.

[31] T. A. Manteuffel and A. B. White, *The numerical solution of second-order boundary value problems on non-uniform meshes*, Mathematics of Computation, 1986, 47, 176, 511–535.

[32] J. J. H. Miller, E. O'Riordan and G. I. Shishkin, *Fitted Numerical Methods for Singular Perturbation Problems*, World Scientific, Singapore, 2012.

[33] R. C. Mittal and G. Arora, *Numerical solution of the coupled viscous Burger-s' equation*, Communications in Nonlinear Science and Numerical Simulation, 2011, 16(3), 1304–1313.

[34] R. K. Mohanty and N. Setia, *A new high accuracy two-level implicit off-step discretization for the system of two space dimensional quasi-linear parabolic partial differential equations*, Applied Mathematics and Computation, 2012, 219(5), 2680–2697.

[35] R. K. Mohanty and S. Singh, *A new two-level implicit discretization of* $O(k^2 + kh^2 + h^4)$ *for the solution of singularly perturbed two-space dimensional non-linear parabolic equations*, Journal of Computational and Applied Mathematics, 2007, 208(2), 391–403.

[36] A. Mohebbi and Z. Faraz, *Solitary wave solution of nonlinear Benjamin–Bona–Mahony–Burgers equation using a high-order difference scheme*, Computational and Applied Mathematics, 2017, 36, 915–927.

[37] B. J. Noye and H. H. Tan, *Finite difference methods for solving the two-dimensional advection–diffusion equation*, International Journal for Numerical Methods in Fluids, 1989, 9, 75–98.

[38] K. Pan, X. Wu, X. Yue and R. Ni, *A spatial sixth-order CCD-TVD method for solving multidimensional coupled Burgers' equation*, Computational and Applied Mathematics, 2020, 39, 76, 20 pages.

[39] A. D. Polyanin and V. F. Zaitsev, *Handbook of Nonlinear Partial Differential Equations*, CRC Press, Boca Raton, 2004.

[40] H. G. Roos, M. Stynes and L. Tobiska, *Robust Numerical Methods for Singularly Perturbed Differential Equations*, Springer, Berlin, 2008.

[41] V. Rudnev, D. Loveless and R. L. Cook, *Handbook of Induction Heating*, CRC Press, London, 2017.

[42] Y. Saad, *Iterative Methods for Sparse Linear Systems*, SIAM, Philadelphia, 2003.

[43] A. A. Samarskii, P. P. Matus and P. N Vabishchevich, *Difference Schemes with Operator Factors*, Springer, Dordrecht, 2002.

[44] V. K. Saul'yev, *Integration of Equations of Parabolic Type by the Method of Nets*, Elsevier, Amsterdam, 2014.

[45] A. A. Soliman, *On the solution of two-dimensional coupled Burgers equations by variational iteration method*, Chaos, Solitons & Fractals, 2009, 40(3), 1146–1155.

[46] J. C. Strikwerda, *Finite Difference Schemes and Partial Differential Equations*, SIAM, Philadelphia, 2004.

[47] H. Sundqvist and G. Veronis, *A simple finite-difference grid with non-constant intervals*, Tellus, 1970, 22(1), 26–31.

[48] Z. Tian, *A rational high-order compact ADI method for unsteady convection–diffusion equations*, Computer Physics Communications, 2011, 182(3), 649–662.

[49] A. M. Wazwaz, *The tanh method for generalized forms of nonlinear heat conduction and Burgers–Fisher equations*, Applied Mathematics and Computation, 2005, 169(1), 321–338.

[50] J. Zhang and G. Yan, *A lattice Boltzmann model for the Burgers–Fisher equations*, Chaos: An Interdisciplinary Journal of Nonlinear Science, 2010, 20(2), Article ID 023129, 12 pages.